

This is the accepted manuscript made available via CHORUS. The article has been published as:

High-spin mesons below 3 GeV

Cheng-Qun Pang, Bo Wang, Xiang Liu, and Takayuki Matsuki

Phys. Rev. D **92**, 014012 — Published 9 July 2015

DOI: [10.1103/PhysRevD.92.014012](https://doi.org/10.1103/PhysRevD.92.014012)

High-spin mesons below 3 GeV

Cheng-Qun Pang^{1,2,*}, Bo Wang^{1,2,†}, Xiang Liu^{1,2,‡},§ and Takayuki Matsuki^{3,4,¶}

¹*School of Physical Science and Technology, Lanzhou University, Lanzhou 730000, China*

²*Research Center for Hadron and CSR Physics, Lanzhou University & Institute of Modern Physics of CAS, Lanzhou 730000, China*

³*Tokyo Kasei University, 1-18-1 Kaga, Itabashi, Tokyo 173-8602, Japan*

⁴*Theoretical Research Division, Nishina Center, RIKEN, Saitama 351-0198, Japan*

In this work, we study the high-spin states with mass below 3 GeV observed in experiments and the analysis of mass spectrum and investigation of strong decay behaviors of the high-spin states are performed. Comparing our results with the experimental data, we can reveal the underlying properties of these high-spin states. What is more important is that in this work we also predict their abundant decay features, which can provide valuable information to further experimental exploration of these high-spin states.

PACS numbers: 14.40.Be, 12.38.Lg, 13.25.Jx

I. INTRODUCTION

In the past decades, the light-flavor meson family has become more and more abundant with the experimental progress (see the Particle Data Group (PDG) [1]). Among the observed mesons listed in PDG [1], there is a large amount of high-spin states with spin $J \geq 3$ available (see Table I for more details). Although 26 high-spin states are collected in PDG, their properties are not well established presently. Hence it is necessary to solve how to categorize these high-spin states into meson families.

To provide a solution to the above problem in studying high-spin states, we need to carry out their systematic and phenomenological investigation by combining it with the present experimental data. For a $q\bar{q}$ meson system, the orbital quantum number of a meson is at least $L = 2$ corresponding to D -wave when the spin quantum number is $J = 3$. Thus, the high-spin states under discussion have close relationship to D -wave, F -wave, G -wave and H -wave meson families.

In the following, we first focus on how to categorize these high-spin states into the conventional meson family, where the mass spectrum analysis is performed via the Regge trajectory. Furthermore, we calculate the Okubo-Zweig-Iizuka (OZI)-allowed two-body strong decay widths of these high-spin states, which can further test their possible meson assignments in combination with the present experimental data. Accordingly we predict their abundant decay behaviors, which are important information for experimental exploration of high-spin mesons in future.

This paper is organized as follows. After the brief review, in Sect. II we present experimental and theoretical research status. In Sect. III, we adopt the Regge trajectory and the quark pair creation (QPC) model to study the high-spin states observed. The paper ends with conclusion and discussions in Sect. IV.

II. CONCISE REVIEW OF THE PRESENT RESEARCH STATUS

Before illustrating our calculation, we first give a brief review of the research status of the high-spin states observed, which we hope is convenient for the readers.

A. States with $J = 3$

An obvious peak signal was observed in the reaction $p\bar{p} \rightarrow \eta\pi^0\pi^0, \pi^0\pi^0, \pi^+\pi^-, \eta\eta$, and $\eta\eta'$ [2] which is named as $f_3(2050)$. Another f_3 state $f_3(2300)$ was introduced by performing the partial wave analysis (PWA) of the data of $p\bar{p} \rightarrow \Lambda\bar{\Lambda}$ [3]. In Refs. [2, 4], $f_3(2050)$ was suggested to be a ground state of the F -wave meson family, while $f_3(2300)$ can be its first radial excitation. Different assignments from Ref. [2], $f_3(2050)$ and $f_3(2300)$ as the first and the second radial excitations of the f_3 meson family, were proposed in Ref. [5], where an unobserved ground f_3 state with mass around 1.7 GeV was predicted. Ref. [4] by the similar method and give the same assignment as Ref. [2]. Ebert *et al.* obtained the mass spectrum of some high-spin states via the relativistic quark model based on the quasipotential approach [6], where the mass spectrum calculation shows that $f_3(2300)$ can be a ground state in the f_3 meson family, which has dominant $s\bar{s}$ component.

There are three observed a_3 states. In the process $\pi^-p \rightarrow \pi^+\pi^-\pi^-p$, the E852 experiment reported a resonance $a_3(1875)$, and some ratios were measured. Other two states, $a_3(2030)$ and $a_3(2275)$, were observed in the $p\bar{p}$ annihilation by SPEC [7, 8]. In Ref. [5], the authors suggested that $a_3(1875)$ and $a_3(2030)$ might be the same state, which can be a ground state and $a_3(2275)$ is the first radial excitation in the a_3 family. Additionally, the mass of the $n^{2s+1}L^J = 1^3F_3$ state calculated by the relativistic quark model is 1910 MeV which corresponds to $a_3(1875)$ [6].

The SPEC experiment [9–11] observed $h_3(2025)$, $h_3(2275)$, $b_3(2030)$, and $b_3(2245)$ by analyzing the New Crystal Barrel data in the $p\bar{p}$ annihilation. These papers suggested that $h_3(2275)$ and $b_3(2245)$ are the first radial excitations of $h_3(2025)$ and $b_3(2030)$ which are the ground states in the h_3 and b_3 meson families, respectively. In Refs. [4,

*Corresponding author

*Electronic address: pangchq13@lzu.edu.cn

†Electronic address: wangb13@lzu.edu.cn

‡Electronic address: xiangliu@lzu.edu.cn

¶Electronic address: matsuki@tokyo - kasei.ac.jp

TABLE I: The observed high-spin states collected in PDG [1]. Here, the states listed as further states in PDG are marked by the superscript f. The C parity is valid only for the corresponding neutral states where the J^{PC} quantum numbers of these high-spin states appear with isospin $I = 1$. We need to emphasize that $\rho_3(1690)$, $\rho_3(1990)$, and $\rho_3(2250)$ are not listed here since these three states have been studied in our former work [12]. In the fifth column, we list some branching ratios and decay modes experimentally observed. In this work we adopt an abbreviation, ω , ρ , η' , a_0 , b_1 , f_2 , and a_2 for the $\omega(782)$, $\rho(770)$, $\eta'(958)$, $a_0(980)$, $b_1(1260)$, $f_2(1270)$, and $a_2(1320)$, respectively.

$I(J^{PC})$	State	Mass (MeV)	Width (MeV)	Other information
$0(3^{--})$	$\omega_3(1670)$	1667 ± 4	168 ± 10	$\Gamma_{\omega\pi\pi}/\Gamma_{\rho\pi} = 0.71 \pm 0.27$ [13], πb_1 [14]
$0(3^{--})$	$\omega_3(1945)^f$	1945 ± 20	115 ± 22	$\eta\omega$ [9]
$0(3^{--})$	$\omega_3(2255)^f$	2255 ± 15	170 ± 30	$\eta\omega$ [3, 9]
$0(3^{--})$	$\omega_3(2285)^f$	2278 ± 28	224 ± 50	$\eta\omega$ [3, 9]
$0(3^{--})$	$\phi_3(1850)$	1854 ± 7	87^{+28}_{-23}	$\Gamma_{KK^*}/\Gamma_{KK} = 0.55^{+0.85}_{-0.45}$ [15]
$0(3^{++})$	$f_3(2050)^f$	2048 ± 8	213 ± 34	$[\eta f_2]_{L=1,3}, \pi a_2$ [2]
$0(3^{++})$	$f_3(2300)^f$	2334 ± 2	200 ± 20	$[\eta f_2]_{L=1,3}, \eta' f_2$ [3]
$1(3^{++})$	$a_3(1875)^f$	$1874 \pm 43 \pm 96$	$384 \pm 121 \pm 114$	$\Gamma_{f_2\pi}/\Gamma_{\rho\pi} = 0.8 \pm 0.2$, $\Gamma_{\rho_3(1690)\pi}/\Gamma_{\rho\pi} = 0.9 \pm 0.3$ [16]
$1(3^{++})$	$a_3(2030)^f$	2031 ± 12	150 ± 18	ηa_2 , πf_2 [11]
$1(3^{++})$	$a_3(2275)^f$	2275 ± 35	350^{+100}_{-50}	$a_0\eta$, ηf_2 [11]
$0(3^{+-})$	$h_3(2025)^f$	2025 ± 20	145 ± 30	$\eta\omega$ [9]
$0(3^{+-})$	$h_3(2275)^f$	2275 ± 25	190 ± 45	$\eta\omega$ [9]
$1(3^{+-})$	$b_3(2030)^f$	2032 ± 12	117 ± 11	$\omega\pi^0$, $\pi^+\pi^-$ [10]
$1(3^{+-})$	$b_3(2245)^f$	2245 ± 50	320 ± 70	ωa_2 , $\omega\pi$, $b_1\eta$, $\pi\omega(1650)$ [11]
$0(4^{++})$	$f_4(2050)$	2018 ± 11	237 ± 18	$\Gamma_{\omega\omega}/\Gamma_{\pi\pi} = 1.5 \pm 0.3$ [17], $\Gamma_{\pi\pi}/\Gamma_{Total} = 0.170 \pm 0.015$ [1]
				$\Gamma_{\eta\eta}/\Gamma_{Total} = (2.1 \pm 0.8) \times 10^{-3}$ [18], $\Gamma_{KK}/\Gamma_{\pi\pi} = 0.04^{+0.02}_{-0.01}$ [19]
$0(4^{++})$	$f_4(2300)$	2320 ± 60	250 ± 80	$\Gamma_{\rho\rho}/\Gamma_{\omega\omega} = 2.8 \pm 0.5$ [20], K^+K^- [21], $\pi\pi$ [22, 23], $\eta\eta$ [24], ηf_2 [11]
$1(4^{++})$	$a_4(2040)$	1996^{+10}_{-9}	255^{+28}_{-24}	$\Gamma_{\pi\rho}/\Gamma_{\pi f_2} = 1.1 \pm 0.2 \pm 0.2$ [16], KK [25, 26], $\rho\omega$ [27], $\eta\pi^0$ [7, 28, 29], $\eta'\pi$ [7, 30]
$1(4^{++})$	$a_4(2255)^f$	2237 ± 5	291 ± 12	$\pi\eta$, $\pi\eta'$, πf_2 [11]
$0(4^{+-})$	$\eta_4(2330)^f$	2328 ± 38	240 ± 90	$a_0\pi$ [2], πa_2 [2], ηf_2 [11]
$1(4^{+-})$	$\pi_4(2250)^f$	2250 ± 15	215 ± 25	$a_0\eta$ [11]
$0(4^{--})$	$\omega_4(2250)^f$	2250 ± 30	150 ± 50	$\eta\omega$ [9]
$1(4^{--})$	$\rho_4(2230)^f$	2230 ± 25	210 ± 30	$\omega\pi^0$, $\pi^+\pi^-$ [10]
$0(5^{--})$	$\omega_5(2250)^f$	2250 ± 70	320 ± 95	$\eta\omega$, πb_1 [11]
$1(5^{--})$	$\rho_5(2350)$	2330 ± 35	260 ± 70	$\omega\pi^0$ [10], $\pi\pi$ [10, 22, 23], K^+K^- [31, 32]
$0(6^{++})$	$f_6(2510)$	2469 ± 29	283 ± 40	$\Gamma_{\pi\pi}/\Gamma_{Total} = 0.06 \pm 0.01$ [33]
$1(6^{++})$	$a_6(2450)$	2450 ± 130	400 ± 250	KK [25]

5], it is advised that we regard $h_3(2025)/b_3(2030)$ and $h_3(2275)/b_3(2245)$ as the first and second radial excitations in the h_3/b_3 meson families, where the corresponding ground states were predicted. The $b_1(1640)$ state was predicted in Refs. [34, 35]. The study in Ref. [6] indicates that $h_3(2275)$ and $b_3(2245)$ can be the ground states with a component $s\bar{s}$.

The $\omega_3(1670)$ was first found in the $\pi^+n \rightarrow p3\pi^0$ process [36] and had been studied by other experiments (see the details for the experimental information on $\omega_3(1670)$ listed in PDG [1]). The $\omega_3(1670)$ can decay into $\rho\pi$ and $\pi\omega\pi$. The second radial excitation of ω_3 is $\omega_3(1945)$ which was reported by SPEC [9]. At the same time, they also found $\omega_3(2255)$

and $\omega_3(2285)$, which were later confirmed by RVUE [3] and $\omega_3(1670)$ was suggested to be the ground state of the ω_3 family. Combining the PWA with the $n - M^2$ plot, the authors of Ref. [9] proposed that $\omega_3(1945)$ and $\omega_3(2285)$ are 2^3D_3 and 3^3D_3 states, respectively [9], while $\omega_3(2255)$ is a 3^3G_3 state and Reference [4] suggested $\omega_3(2285)$ could be the 1^3G_3 state. The mass spectrum calculation given in [6] shows that $\omega_3(1945)$ and $\omega_3(2285)$ can be the 1^3G_3 and 2^3G_3 states, respectively.

HBC found $\phi_3(1850)$ in the KK and KK^* channels from the K^-p collision [37]. The $\phi_3(1850)$ was confirmed by OMEGA [38] and LASS [15]. Both the $J - M^2$ plot analysis in Refs.

[5, 34, 35] and calculation of the mass spectrum in [6] show that $\phi_3(1850)$ is a good candidate for the 1^3D_3 state.

B. States with $J = 4$

The Serpukhov-CERN Collaboration [39] and CERN-MUNICH Collaboration [40] observed a peak structure in the processes $\pi^- p \rightarrow n2\pi^0$ and $\pi^- p \rightarrow nK^+K^-$, which was named $f_4(2050)$. Other experiments relevant to the observation of $f_4(2050)$ can be found in PDG [1]. Some observed channels and branching ratios are listed in Table I. CNTR [41] first reported the resonance $f_4(2300)$. In the past decades, it appears in the reactions, $p\bar{p} \rightarrow K^+K^-$ [42], $\pi\pi$ [22, 23, 43], $\eta\pi^0\pi^0$ [2], and $\pi^- p \rightarrow K^+K^-$ [24].

There are some theoretical studies on the properties of the observed f_4 states. The $f_4(2050)$ as a molecule state composed of three ρ mesons [44]. Ebert *et al.* got a 1^3F_4 $q\bar{q}$ state with mass $M = 2018$ MeV and a 2^3F_4 $q\bar{q}$ state with mass $M = 2284$ MeV which correspond to $f_4(2050)$ and $f_4(2300)$, respectively [6]. Many studies also support this assignment [4, 34, 35, 45]. Additionally, in Ref. [5], the Regge trajectory analysis shows that $f_4(2050)$ and $f_4(2300)$ are the ground states dominated by the $q\bar{q}$ and $s\bar{s}$ components, respectively.

There are many experiments relevant to $a_4(2040)$. OMEGA observed a resonance with mass around 2030 MeV by the PWA of $\pi^- p \rightarrow n3\pi$ [46]. Later, $a_4(2040)$ was also found in the reactions, $\pi p \rightarrow K_s K^\pm p$ [25], $\pi^- p \rightarrow \eta\pi^0 n$ [29], $\pi^- A \rightarrow \omega\pi^-\pi^0 A^*$ [47], $\pi^- p \rightarrow \eta'\pi^- p$ [30], $\pi^- p \rightarrow \omega\pi^-\pi^0 p$ [27], and $\pi^- P_b \rightarrow \omega\pi^-\pi^+\pi^- P_b$ [27]. The observed decay modes are listed in Table I. In addition, SPEC also reported $a_4(2255)$ in $p\bar{p} \rightarrow \pi^0\eta, 3\pi^0, \pi^0\eta'$ [7]. E835 confirmed the state $a_4(2255)$ in the reaction $p\bar{p} \rightarrow \eta\eta\pi^0$ [28]. All Regge trajectory studies show that $a_4(2040)$ is the ground state of the a_4 family, and $a_4(2255)$ is its first radial excitation [4, 5, 34, 35, 45]. Ebert *et al.* got a 1^3H_4 state with mass $M = 2234$ MeV which is very close to $a_4(2255)$ [6]. However, in Ref. [7], the PWA shows that $a_4(2255)$ is a 3^3F_4 state.

In the reactions $p\bar{p} \rightarrow \eta\pi^0\pi^0, \pi^0\pi^0, \pi^+\pi^-, \eta\eta, \eta\eta'$, SPEC reported a 1^3G_4 state with the mass 2328 ± 38 MeV and width 240 ± 90 MeV in the final states $(\pi a_2)_{L=4}$ and $(\pi a_0)_{L=4}$, where $L = 4$ denotes G -wave [2], which was named $\eta_4(2330)$. They also reported the resonance $\pi_4(2250)$ in the $p\bar{p}$ annihilation through studying the Crystal Barrel data [7]. The Regge trajectory analysis shows that both $\pi_4(2250)$ and $\eta_4(2330)$ are the ground states in the π_4 and η_4 families [4, 5, 34, 35] with different isospins $I = 1$ and 0 , respectively. The study of mass spectrum of high-spin states in Ref. [6] indicates that $\pi_4(2250)$ and $\eta_4(2330)$ are the first radial excitations of G -wave mesons, where mass 2092 MeV for the corresponding ground states was predicted.

$\omega_4(2250)$ [9] and $\rho_4(2230)$ [10] was reported by SPEC. Both the mass spectrum calculation in Ref. [6] and the $J - M^2$ plot in Ref. [4, 5] support that $\omega_4(2250)$ and $\rho_4(2230)$ are the 1^3G_4 states with different isospins as above.

C. States with $J = 5$

Analyzing the $\eta\omega$ and $\omega\pi^0\pi^0$ data, SPEC strongly requires a 3^3G_5 state around 2250 MeV [9], which corresponds to $\omega_5(2250)$. Later, the mass error of $\omega_5(2250)$ was given in Ref. [11].

An isospin $I = 1$ and $J = 5$ structure $\rho_5(2350)$ was observed in the $p\bar{p}$ total cross section [31]. It can decay into $\omega\pi^0, \pi^+\pi^-, \pi^0\pi^0$, and K^+K^- [10, 22, 23, 32, 42, 48, 49].

The present theoretical studies support $\omega_5(2250)$ as a ground state [5, 6]. The $\rho_5(2350)$ is also a ground state, which was suggested in Refs. [4–6, 34, 35, 45]. However, the authors of Ref. [44] treated $\rho_5(2350)$ as a molecule of four ρ mesons.

D. States with $J = 6$

GAM2 observed a $J = 6$ neutral meson $R(2510)$ [33] which is now named $f_6(2510)$ due to the contribution by Ref. [50], where the branching ratio of its $\pi\pi$ mode was given. The $f_6(2510)$ was confirmed in the reaction $\pi^- p \rightarrow 2\pi^0 n$ [51] and SPEC also found it in the $p\bar{p}$ annihilation [2].

There is only one experiment about $a_6(2450)$ which was observed by SPEC in the reaction $\pi p \rightarrow K_s^0 K^\pm p$ [52].

From the mass spectrum analysis in Refs. [6, 34, 35], the $f_6(2510)$ is a good candidate of the 1^3H_6 $q\bar{q}$ state. The $a_6(2450)$ is the isospin partner of $f_6(2510)$ [5, 6, 34, 35, 45]. A different explanation for $f_6(2510)$, i.e., a molecular state of five ρ mesons, was proposed in Ref. [44].

From the above review, we can find that the present status of the high-spin states is still in disorder, where different groups gave different theoretical explanations. This situation inspires us to carry out a systematic study of these high-spin states, which can improve our understanding of the properties of these states.

III. PHENOMENOLOGICAL ANALYSIS

The phenomenological analysis presented in this work includes two methodologies. First, the analysis of Regge trajectories is adopted to study possible meson assignments to the high-spin states under discussion. Secondly, we use the QPC model to obtain their OZI-allowed two-body decay behaviors. In the following, we give a brief introduction to these methods adopted.

The analysis of Regge trajectory provides a general method to study the meson spectrum [45]. The excited states and ground states satisfy a simple relation

$$M^2 = M_0^2 + \mu^2(n-1), \quad (1)$$

where M_0 and M are the masses of ground state and excited state, respectively. The μ^2 gives a slope of a trajectory with the value $\mu^2 = 1.25 \pm 0.15$ GeV² suggested in Ref. [45]. Via the above equation, we obtain the $n - M^2$ plot of the mesons under discussion, where the radial quantum number n of these states

can be obtained when mass is given, which is the important information of the underlying structure of mesons.

Besides the relation in Eq. (1), there exists a similar relation

$$M_J^2 = M_{J'}^2 + \alpha^2(J - J'), \quad (2)$$

where J or J' denotes the spin of a meson. $M_{J'}$ and M_J are the masses of mesons with different spins and with the same P and C quantum numbers. Via Eq. (2), the corresponding J - M_J^2 plot can be obtained, which provides an extra test of the conclusion from the n - M^2 plot.

When further checking the relation of masses of high-spin mesons with the principle quantum number $N = n + J$, we find that there exists the symmetry of the spectrum in the form

$$M_N^2 = M_0^2 + \beta^2 N, \quad (3)$$

where this phenomenon argues in favor of the existence of the principle quantum which governs the spectrum of excited mesons just indicated in Refs. [53, 56].

In the following, we briefly explain the QPC model adopted in this work. After the QPC model was proposed by Micu [57], this model was further developed by the Orsay group [58–62]. Later, this model was widely applied to study the OZI-allowed strong decay of hadrons [12, 63–79].

For a two-body strong decay process $A \rightarrow B + C$, the corresponding transition matrix element can be written as

$$\langle BC|T|A \rangle = \delta^3(\mathbf{P}_B + \mathbf{P}_C) \mathcal{M}^{M_{J_A} M_{J_B} M_{J_C}}, \quad (4)$$

where $\mathbf{P}_{B(C)}$ denotes the three-momentum of a final particle $B(C)$. M_{J_i} ($i = A, B, C$) is an orbital magnetic momentum of the corresponding meson in the decay. $\mathcal{M}^{M_{J_A} M_{J_B} M_{J_C}}$ is the amplitude we calculate. The T operator reads as

$$T = -3\gamma \sum_m \langle 1m; 1 - m | 00 \rangle \int d\mathbf{p}_3 d\mathbf{p}_4 \delta^3(\mathbf{p}_3 + \mathbf{p}_4) \times \mathcal{Y}_{1m} \left(\frac{\mathbf{p}_3 - \mathbf{p}_4}{2} \right) \chi_{1,-m}^{34} \phi_0^{34} \left(\omega_0^{34} \right)_{ij} b_{3i}^\dagger(\mathbf{p}_3) d_{4j}^\dagger(\mathbf{p}_4), \quad (5)$$

where γ is a parameter which takes the value 8.7 or $8.7/\sqrt{3}$ when the quark-antiquark pair created from the vacuum is $u\bar{u}(d\bar{d})$ or $s\bar{s}$ [77]. The quark and anti-quark created from the vacuum are marked by the subscripts 3 and 4, respectively. i/j denotes the color indexes. The χ , ϕ , and ω are the spin, flavor and color wave functions, respectively. In addition, $\mathcal{Y}_{\ell m}(\mathbf{p}) = |\mathbf{p}|^\ell Y_{\ell m}(\mathbf{p})$ is the solid harmonic polynomial (see Refs. [80, 81] for more details). Using the Jacob-Wick formula [82], the amplitude $\mathcal{M}^{M_{J_A} M_{J_B} M_{J_C}}$ can be converted into the partial wave amplitude $M^{JL}(\mathbf{P})$, i.e.,

$$\mathcal{M}^{JL}(\mathbf{P}) = \frac{\sqrt{4\pi(2L+1)}}{2J_A+1} \sum_{M_{J_B} M_{J_C}} \langle L0; J M_{J_A} | J_A M_{J_A} \rangle \times \langle J_B M_{J_B}; J_C M_{J_C} | J_A M_{J_A} \rangle \mathcal{M}^{M_{J_A} M_{J_B} M_{J_C}}. \quad (6)$$

Finally, the decay width can be given by

$$\Gamma = \frac{\pi |\mathbf{P}|}{4m_A^2} \sum_{J,L} |M^{JL}(\mathbf{P})|^2, \quad (7)$$

where m_A is the mass of the initial meson A . In the concrete calculation, we use the harmonic oscillator wave function to describe the meson spatial wave function. The harmonic oscillator wave function has the following expression $\Psi_{nlm}(R, \mathbf{p}) = \mathcal{R}_{nl}(R, \mathbf{p}) \mathcal{Y}_{lm}(\mathbf{p})$, with R being a parameter, which is given in Ref. [68] for the mesons involved in our calculation.

Before performing the phenomenological analysis of these high-spin mesons, we need to emphasize that the orbital quantum number for these discussed high-spin mesons with $J^{PC} = 3^{--}, 4^{++}, 5^{--}$, and 6^{++} cannot be fixed just indicated in Refs. [53–55]. For example, the meson with $J^{PC} = 3^{--}$ is the mixture between the $L = 2$ and $L = 4$ states¹. By our calculation, we find that the contribution of the higher orbital quantum number for these high-spin mesons with $J^{PC} = 3^{--}, 4^{++}, 5^{--}$, and 6^{++} is far smaller than that of the lower orbital quantum number when we study their decay behavior. Thus, in the following, we will only consider contribution from the lower orbital quantum number for these discussed high-spin mesons with $J^{PC} = 3^{--}, 4^{++}, 5^{--}$, and 6^{++} .

A. Twelve J^{--} states

In this subsection, we discuss twelve observed high-spin states with the J^{--} ($J = 3, 4, 5$) quantum numbers (see Table I). The corresponding analysis of Regge trajectories with the n - M^2 and J - M^2 plots are shown in Fig. 1.

There are eight high-spin states with $J^{PC} = 3^{--}$, which are $\omega_3(1670)$, $\omega_3(1945)$, $\omega_3(2255)$, $\omega_3(2285)$, $\phi_3(1850)$, $\rho_3(1690)$, $\rho_3(1990)$, and $\rho_3(2250)$. As an effective approach to study the meson categorization, analysis of the Regge trajectory is applied to further discuss the $\omega_3(1670)$, $\omega_3(1945)$, $\omega_3(2255)$, $\omega_3(2285)$, and $\phi_3(1850)$. In Ref. [12], the properties of $\rho_3(1690)$, $\rho_3(1990)$, and $\rho_3(2250)$ were studied, where they can be explained as $n^3 D_3$ ($n = 1, 2, 3$) states in the ρ_3 meson family, respectively. In Fig. 1 (a), we make a comparison of the observed ω_3 and ρ_3 states, which reflects the similarity between ρ_3 and ω_3 meson families because of their similar values of the slope μ^2 . Thus, we can conclude that $\omega_3(1670)$, $\omega_3(1945)$, and $\omega_3(2285)$ are the isospin partners of $\rho_3(1690)$, $\rho_3(1990)$, and $\rho_3(2250)$, respectively.

As shown in Fig. 1 (b), we also give the J - M^2 plot analysis, which also supports the assignments of $\omega_3(1670)$, $\omega_3(1945)$, and $\omega_3(2285)$ as the ground, the first, and the second radial excitations, respectively. In addition, the J - M^2 analysis also indicates that $\phi_3(1850)$ is the ground state in the ϕ_3 meson family.

The partial wave analysis in Ref. [9] indicates that $\omega_3(2255)$ is a G-wave meson. Furthermore, $\omega_3(2255)$ corresponds to $\omega_3(1^3 G_3)$ since this assignment is supported by the J - M^2 plot

¹ The meson with $J^{PC} = 4^{++}$ is the mixture between the $L = 3$ and $L = 5$ states, while the meson with $J^{PC} = 5^{--}$ is from the mixture between the $L = 4$ and $L = 6$ states. In addition, the meson with $J^{PC} = 6^{++}$ is due to the mixture between the $L = 5$ and $L = 7$ states

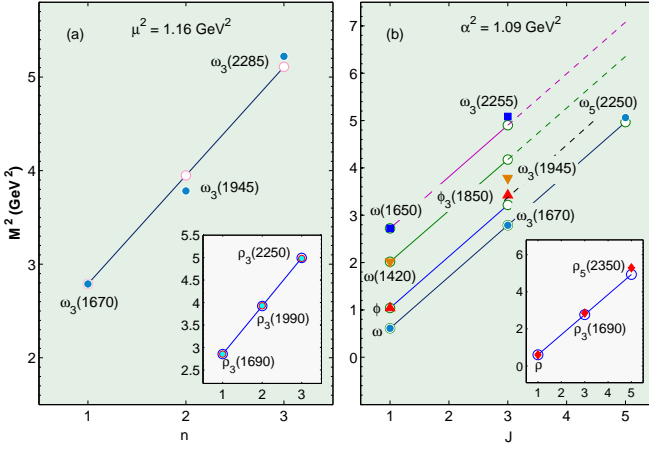


FIG. 1: (color online). Analysis of Regge trajectories for the observed states with the J^- quantum numbers. The diagram (a) is the $n-M^2$ plots for ω_3 and ρ_3 states, while the diagram (b) is the corresponding $J-M^2$ plots for ω , ϕ , and ρ . Here, open and filled circles are the theoretical and experimental values, respectively; $\rho(770)$, $\omega(782)$ and $\phi(1020)$ are abbreviated as ρ , ω and ϕ , respectively, which are adopted in the following figures.

in Fig. 1 (b). Later, we will discuss the decay behavior of $\omega_3(2255)$ with this assignment.

We notice that the mass $\omega_4(2250)$ is close to that of $\rho_4(2230)$, which shows that it is reasonable to assign $\omega_4(2250)$ as the isospin partner of $\rho_4(2230)$. In this work, $\omega_4(2250)$ and $\rho_4(2230)$ are treated as $\omega_4(1^3G_4)$ and $\rho_4(1^3G_4)$, respectively.

According to the $J-M^2$ plot shown in Fig. 1 (b), we can conclude that $\omega_5(2250)$ and $\rho_5(2350)$ are the meson with quantum number 1^3G_5 .

In the following, we further present the study of their two-body OZI-allowed decays.

1. $\omega_3(1670)$, $\omega_3(1945)$, $\omega_3(2255)$, $\omega_3(2285)$, and $\phi_3(1850)$

As for $\omega_3(1670)$, its two-body OZI-allowed strong decays with a 1^3D_3 assignment are given in Fig. 2. When taking $R = 4.0 - 5.4 \text{ GeV}^{-1}$, our theoretical result overlaps with the experimental width of $\omega_3(1670)$ [83]². Here, $\pi\rho$ and πb_1 are main decay modes of $\omega_3(1670)$, which is consistent with the experimental observation since $\pi\rho$ and $\pi\omega\pi$ channels were reported in experiment and $b_1(1235)$ dominantly decays into $\pi\omega$. In summary, $\omega_3(1670)$ as $\omega_3(1^3D_3)$ meson is possible, which was treated in Refs. [3, 5, 34, 84].

Under the 2^3D_3 state assignment, we present the decay

behavior of $\omega_3(1945)$ in Fig. 2. The obtained total decay width can reproduce the experimental width of $\omega_3(1945)$ measured in Ref. [9] if $R = 4.5 - 4.7 \text{ GeV}^{-1}$. Our results also show that $\pi\rho$, πb_1 , and $\eta\omega$ are its main decay channels, where $\omega_3(1945) \rightarrow \eta\omega$ was reported in Ref. [9]. Thus, we suggest further experimental search for its main decay channels $\pi\rho$ and πb_1 , which will be useful to test the underlying structure of $\omega_3(1945)$.

The decay properties of $\omega_3(2285)$ are given in Fig. 2. When taking $R = 4.7 - 5.0 \text{ GeV}^{-1}$, our theoretical results are consistent with the measured experimental width [9]. In addition, $\omega_3(2285)$ mainly decays into $\pi\rho$, πb_1 , and $\eta\omega$, which can explain why $\omega_3(2285)$ was first observed in the $\eta\omega$ channel [9]. Experimental exploration on $\omega_3(2285)$ via the remaining several main decay modes predicted in this work is still an interesting issue.

The above studies indicate that description of $\omega_3(1670)$, $\omega_3(1945)$, and $\omega_3(2285)$ as the ground state, the first and the second radial excitations, respectively, should be further tested.

Next, we illustrate the decay behaviors of $\omega_3(2255)$ under the $\omega_3(1^3G_3)$ assignment (see Fig. 3 for the details). ρa_1 , πb_1 , $\eta\omega$, and ρa_2 are its dominant decay channels. Additionally, the channels ωf_2 , and ηh_1 also mainly contribute to the total width. These quantitative predictions can be served as further experimental investigation of $\omega_3(2255)$. We need to specify that the obtained total decay width is strongly depend on the range of R value. There was an experimental data of the width of $\omega_3(2255)$ given by Ref. [9], which can be reproduced by our calculation with $R \sim 7 \text{ GeV}^{-1}$. For the experimental study of $\omega_3(2255)$, a crucial task is the precise measurement of its resonance parameter, which can provide more abundant information to identify $\omega_3(2255)$ as the 1^3G_3 assignment.

There is only one ϕ_3 state listed in PDG, i.e., $\phi_3(1850)$. We calculate its two-body decays under the $\phi_3(1^3D_3)$ assignment, which are listed in Fig. 3. Here, K^*K^* , KK^* , KK and $KK_1(1270)$ are main decay modes of $\phi_3(1850)$. We notice that experimental data of ratio $\Gamma_{KK^*}/\Gamma_{KK} = 0.55^{+0.85}_{-0.45}$ [15], which shows that the partial width of KK mode is larger than that of the KK^* mode. However, our result shows that the partial width of KK mode is smaller than that of the KK^* mode for $\phi_3(1850)$ since we obtain $\Gamma_{KK^*}/\Gamma_{KK} = 3.5 - 18$. Our conclusion of the KK and KK^* channels is also supported by the study presented in Ref. [85], where the authors obtained $\Gamma_{KK} = 43 \pm 4 \text{ MeV}$ and $\Gamma_{KK^*} = 55 \pm 10 \text{ MeV}$. Since there is only one experimental measurement for this ratio at present, we expect future experiments to clarify the above inconsistency between theoretical and experimental results. Additionally, when we take $R = 5.3 - 7.0 \text{ GeV}^{-1}$, we can find a common range where the theoretical result is consistent with the experimental width given in Ref. [38].

2. $\omega_4(2250)$, $\rho_4(2230)$, $\omega_5(2250)$ and $\rho_5(2350)$

As the candidates of $\omega_4(1^3G_4)$ and $\rho_4(1^3G_4)$, $\omega_4(2250)$ and $\rho_4(2230)$ have the decay behaviors listed in Fig. 4, respectively. By this study, we conclude that ρa_1 , ρa_2 , and $\pi\rho$

² Just shown in PDG [1], different experiments gave different results of the width of $\omega_3(1670)$. When comparing our calculation with experimental data, we adopt the result in Ref. [83] since the corresponding R value is reasonable. In the following discussion, we notice the adopted R ranges for $\omega_3(1945)$ and $\omega_3(2285)$, which satisfy the requirement that the R range becomes more larger with increasing the radial quantum number.

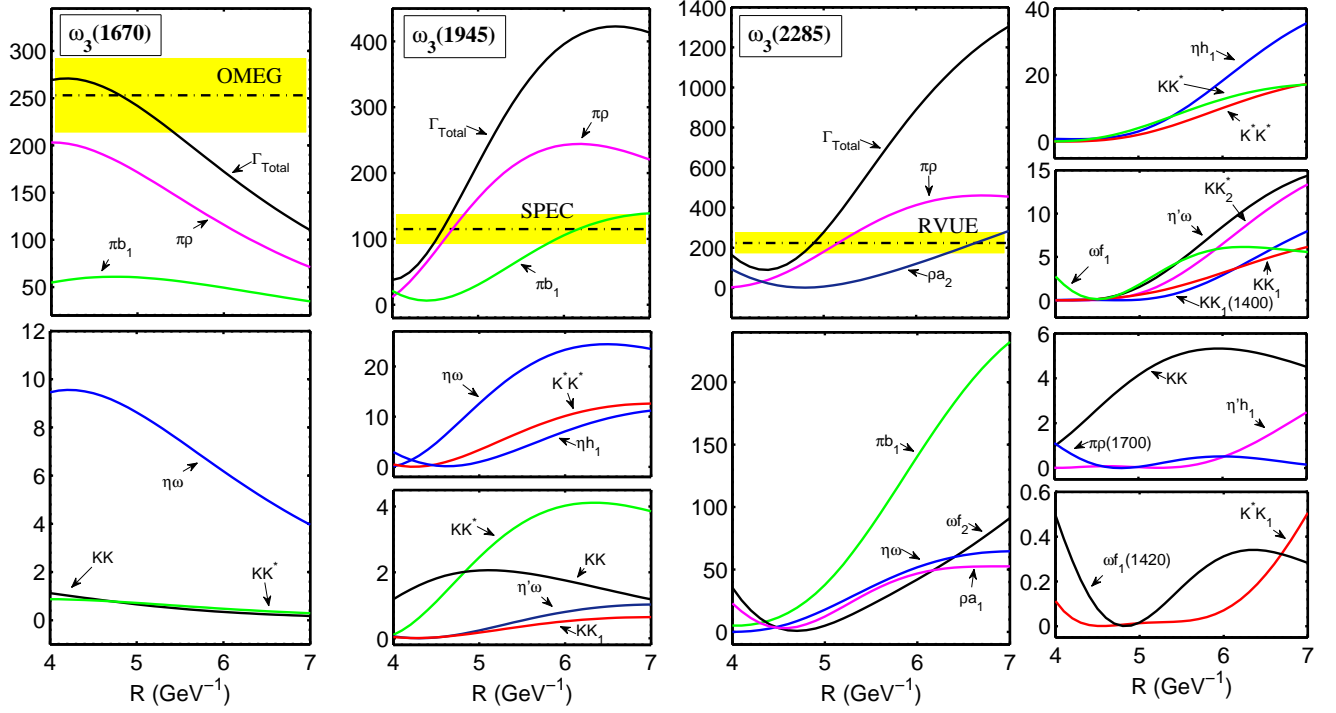


FIG. 2: (color online). The R value dependence of the partial and total decay widths of $\omega_3(1670)$, $\omega_3(1945)$, and $\omega_3(2285)$. All results are in units of MeV. The dot-dashed lines with yellow bands are the corresponding experimental widths of $\omega_3(1670)$ [83], $\omega_3(1945)$ [9], and $\omega_3(2285)$ [9]. Here, $a_1(1260)$, $h_1(1170)$, $f_1(1285)$, $K^*(892)$, $K_1(1270)$, and $K_2^*(1430)$ are abbreviated as a_1 , h_1 , f_1 , K^* , K_1 , and K_2^* , respectively, which are also adopted in the following figures.

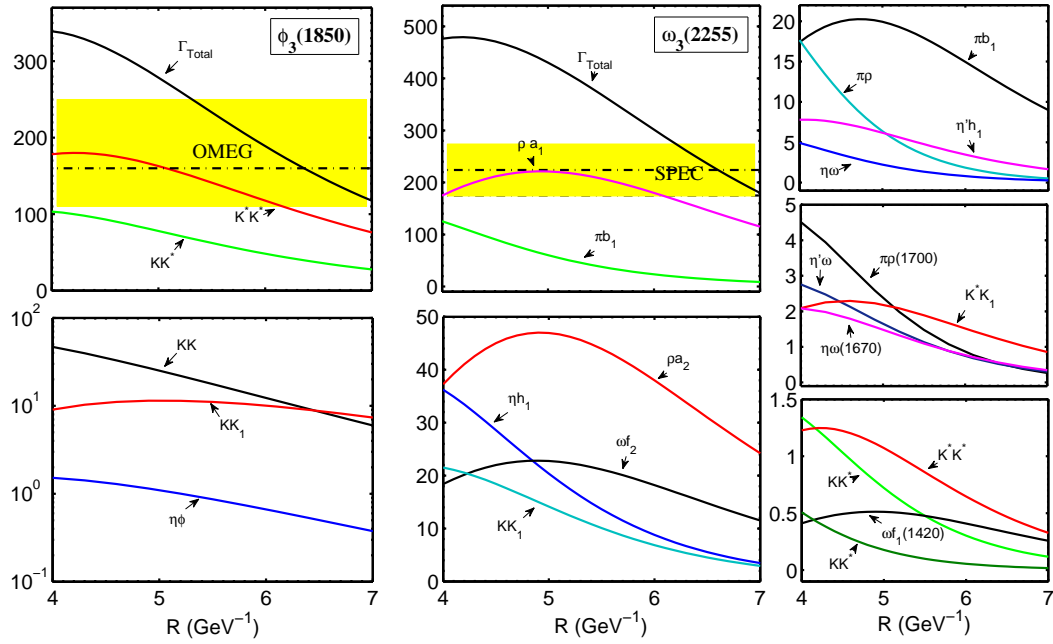


FIG. 3: (color online). The R value dependence of the partial and total decay widths of the $\omega_3(2255)$ and $\phi_3(1850)$ under discussion. All results are in units of MeV. The dot-dashed lines with yellow bands are the corresponding experimental widths of $\omega_3(2255)$ [9] and $\phi_3(1850)$ [38].

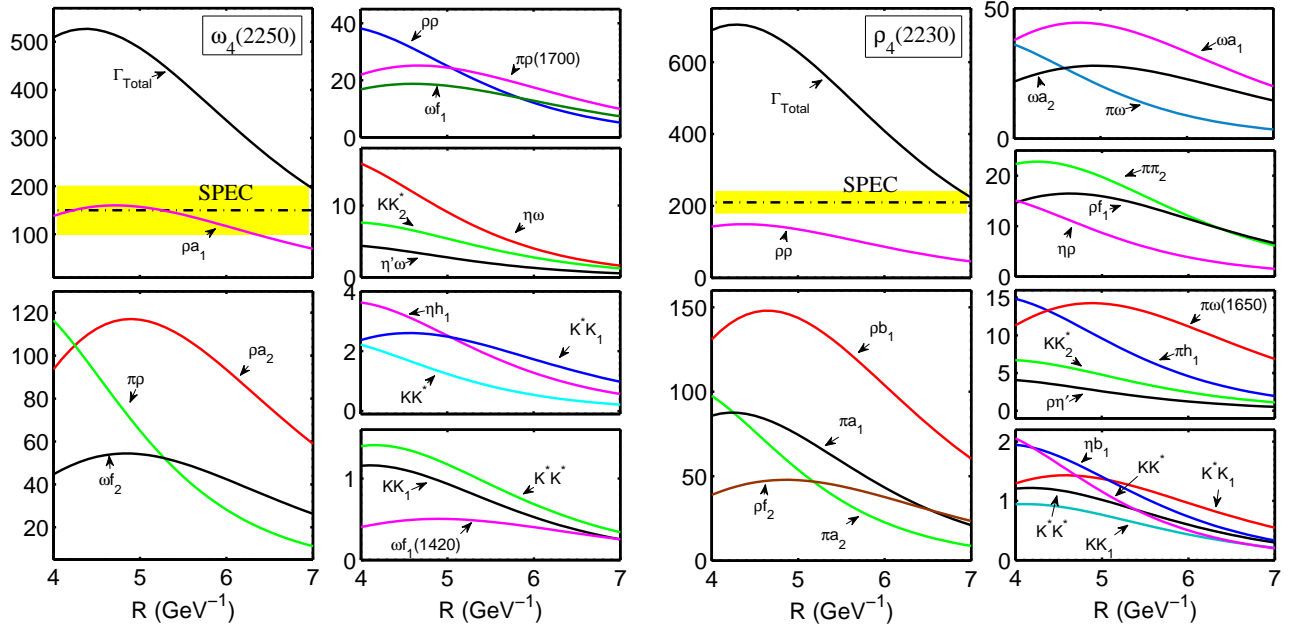


FIG. 4: (color online). The R value dependence of the partial and total decay widths of $\omega_4(2250)$ and $\rho_4(2230)$. All results are in units of MeV. The dot-dashed lines with yellow bands denote the corresponding experimental widths of $\omega_4(2250)$ [9] and $\rho_4(2230)$ [10]. Here, $\pi_2(1670)$ is abbreviated as π_2 .

are main decay modes of $\omega_4(2250)$, while $\rho_4(2230)$ mainly decays into $\rho\rho$, ρb_1 , πa_2 , and πa_1 . At present, the experimental information of $\omega_4(2250)$ and $\rho_4(2230)$ is still scarce. For example, there is only one experimental measurement for the width of $\omega_4(2250)$ or $\rho_4(2230)$. When $R \approx 7 \text{ GeV}^{-1}$ is adopted, theoretical total decay widths can overlap with the experimental data for $\omega_4(2250)$ [9] and $\rho_4(2230)$ [10].

Both $\omega_5(2250)$ and $\rho_5(2350)$ are good candidate of G-wave mesons. In Fig. 5, we present their decay features. Here, the main decay modes of $\omega_5(2250)$ include ρa_2 , ωf_2 , πb_1 and $\pi\rho$, among which πb_1 was reported in experiment [86]. As for $\rho_5(2350)$, ρf_2 and ωa_2 are its dominant decay modes, while $\rho\rho$, πa_2 and πh_1 are also important contributions to the total decay width. Since the experimental status of $\omega_5(2250)$ and $\rho_5(2350)$ is similar to that of $\omega_4(2250)$ and $\rho_4(2230)$, where there is not enough information of their experimental data. Thus, we compare the obtained total widths of $\omega_5(2250)$ and $\rho_5(2350)$ with the present experimental data [49, 86] (see Fig. 5 for more details).

These theoretical predictions of the decay behaviors of $\omega_4(2250)$, $\rho_4(2230)$, $\omega_5(2250)$ and $\rho_5(2350)$ are useful for their experimental studies in future.

B. Eleven J^{++} states

As listed in Table I, eleven high-spin states with the J^{++} ($J = 3, 4, 6$) quantum numbers were reported in experiments. In Fig. 6, we present the systematic analysis of Regge trajectories with the $n-M^2$ and $J-M^2$ plots, which is helpful to obtain the information of their classification into meson families.

Fig. 6 (a) shows that $f_3(2050)$ is the ground state of the f_3 family, while $f_3(2300)$ is the radial excitation, which is in good agreement with the conclusion in Refs. [2, 4]. As the isospin partners of $f_3(2050)$ and $f_3(2300)$, $a_3(2030)$ and $a_3(2275)$ are the ground state and the first radial excitation in the a_3 meson family, respectively, which is reflected in Fig. 6 (a). In addition, we notice that there is the $a_3(1875)$, which cannot be categorized into the a_3 meson family. Thus, in the following discussion of their decay behaviors, we will mainly focus on $f_3(2050)$, $f_3(2300)$, $a_3(2030)$, and $a_3(2275)$.

When checking $a_4(2040)$, $a_4(2255)$, and their isospin partners $f_4(2050)$ and $f_4(2300)$, we conclude that $a_4(2040)/f_4(2050)$ and $a_4(2255)/f_4(2300)$ are the ground state and the first radial excitation in the a_4/f_4 meson families, respectively, which can be supported by the analysis of the $n-M^2$ and $J-M^2$ plots shown in Fig. 6.

From the analysis shown in Fig. 6, we can draw a conclusion that $f_6(2510)$ is a candidate of the $f_6(1^3H_6)$ meson and that $a_6(2450)$ is the isospin partner of $f_6(2510)$.

In the following, we further test the above meson assignments to the states with J^{++} quantum numbers under discussion by carrying out the study of their two-body OZI-allowed strong decays.

1. $f_3(2050)$, $f_3(2300)$, $a_3(2030)$, and $a_3(2275)$

In Figures 7-9, the decay behaviors of $f_3(2050)$, $f_3(2300)$, $a_3(2030)$, and $a_3(2275)$ are given, where their partial and total decay widths are obtained by the QPC model. In addition, we also compare our results with the experimental data.

$f_3(2050)$ and $f_3(2300)$ are treated as $f_3(1^3F_3)$ and $f_3(2^3F_3)$ with isospin $I = 0$, respectively. As for $f_3(2050)$, our calculation indicates that $\rho\rho$, πa_2 , ρb_1 , πa_1 are its main decay channels, and $f_3(2050) \rightarrow \eta f_2$ is sizable contribution to its total decay width, which can explain why the experiment reported $f_3(2050)$ in its πa_2 and ηf_2 decay modes. However, the obtained total decay width of $f_3(2050)$ is far larger than the experimental width given in Ref. [2] when taking $R = 4 - 7 \text{ GeV}^{-1}$. As for $f_3(2300)$, its main decay channels include $\rho\rho$, ρb_1 , $\pi\pi_2$, and $\omega\omega$. The calculated total decay width of $f_3(2300)$ is also larger than the experimental data [2] (see Fig. 7). To some extent, the situation of $f_3(2050)$ is similar to that of $f_3(2300)$. To further clarify the above inconsistency between an experimental width and the theoretical result, further experimental measurement of $f_3(2050)$ and $f_3(2300)$ is encouraged.

Before illustrating the decay properties of $a_3(2030)$, and $a_3(2275)$ which are the isospin partners of $f_3(2050)$ and $f_3(2300)$, we still need to discuss $a_3(1875)$. Although $a_3(1875)$ cannot be grouped into the a_3 meson family only in term of the analysis of the Regge trajectories, the authors in Ref. [5] suggest that $a_3(1875)$ and $a_3(2030)$ are the same state. If $a_3(1875)$ is $a_3(1^3F_3)$, our calculated results of the branching ratio of $B(a_3(1875) \rightarrow f_2(1270)\pi)/B(a_3(1875) \rightarrow \pi\rho)$ is about 1, which is consistent with the experimental data 0.8 ± 0.2 given in Ref. [16]. Additionally, $B(a_3(1875) \rightarrow \rho_3(1690)\pi)/B(a_3(1875) \rightarrow \pi\rho)$ in Ref. [16] is about 0.9 ± 0.3 , where our calculation gives $1.9 - 2.4$ for this ratio. Thus, the $a_3(1^3F_3)$ assignment to $a_3(1875)$ seems to be reasonable. Thus, measuring the resonance parameters of $a_3(1875)$ and $a_3(2030)$ is a crucial task to test whether $a_3(1875)$ and $a_3(2030)$ are the same state.

$a_3(2030)$ mainly decays into $\rho\omega$, $\pi\rho$, and ρh_1 , and ηa_2 and πf_2 sizably contribute to the total width. Here, the $a_3(2030)$ decays into ηa_2 and πf_2 were observed in experiment [1]. The theoretical total decay width of $a_3(2030)$ with the range $R = 4 - 7 \text{ GeV}^{-1}$ is far larger than the experimental measurement [7]. Under the $a_3(1^3F_3)$ meson assignment, $a_3(2275)$ has main decay modes $\rho\omega$, ρa_1 , and $\pi\rho$. Fig. 8 displays the R dependence of the partial decay width of $a_3(2275)$, which shows that the calculated total width overlaps with the experimental data [8] when $R = 4.6 - 5 \text{ GeV}^{-1}$.

2. $f_4(2050)$, $f_4(2300)$, $a_4(2040)$, and $a_4(2255)$

In this subsection, we present the decay properties for four 4^{++} states $f_4(2050)$, $f_4(2300)$, $a_4(2040)$, and $a_4(2255)$, which are shown in Fig. 9-10.

The results of $f_4(2050)$ shown in Fig. 9 indicate that $\rho\rho$, πa_2 , and $\omega\omega$ are its dominant decay channels. Furthermore, we also get some typical ratios, which are comparable with

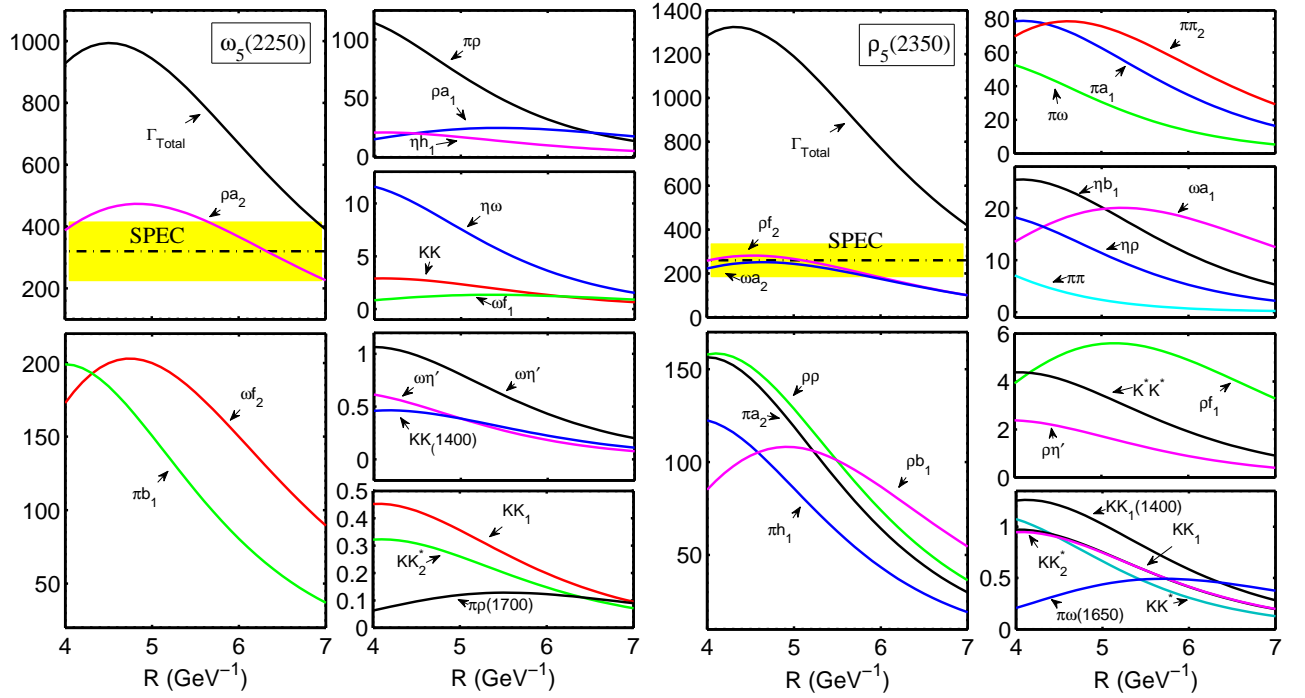


FIG. 5: (color online). The R value dependence of the partial and total decay widths of $\omega_5(2250)$ and $\rho_5(2350)$ states. All results are in units of MeV. The dot-dashed lines with yellow bands are experimental widths of $\omega_5(2250)$ [86] and $\rho_5(2350)$ [49].

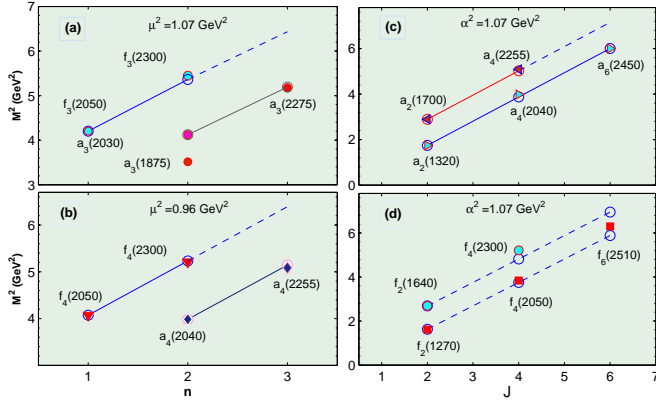


FIG. 6: (color online). The analysis of Regge trajectories for the observed states with the J^{++} quantum numbers. Diagrams (a) and (b) are the n - M^2 plots for the 3^{++} and 4^{++} states, respectively, while diagrams (c) and (d) are the corresponding J - M^2 plots. For diagrams (a) and (b), the $I = 1$ n - M^2 trajectories are displaced one unit to the right in n in order to resolve them from $I = 0$.

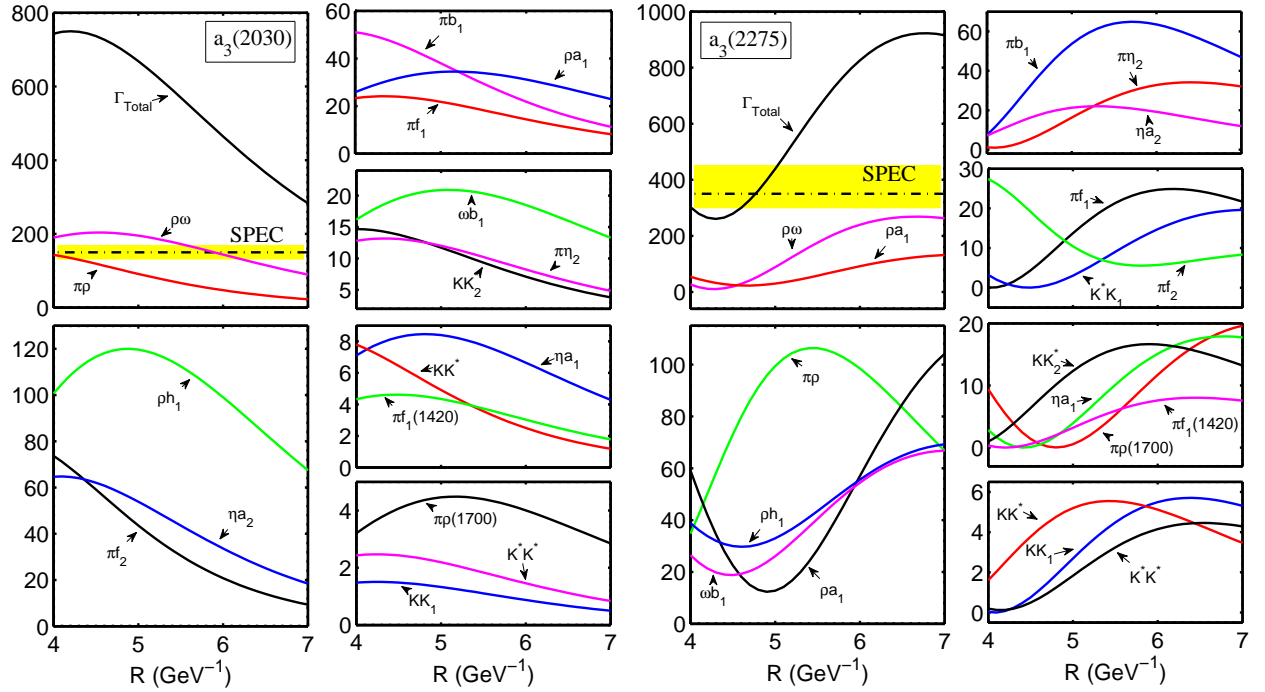
the experimental data (see Table II for more details). As for $f_4(2300)$, πa_2 and $\rho\rho$ are its dominant decay channels, and the obtained ratio $\Gamma_{f_4(2300) \rightarrow \rho\rho} / \Gamma_{f_4(2300) \rightarrow \omega\omega} = 0.6 - 3.1$ is consistent with the experimental value 2.8 ± 0.5 [20]. The total decay widths of $f_4(2050)$ and $f_4(2300)$ overlap with the corresponding experimental widths when $R = 4 - 7 \text{ GeV}^{-1}$. Thus, these studies support $f_4(2050)$ and $f_4(2300)$ as the candidates

TABLE II: Comparison between the calculated and experimental results for some typical ratios of $f_4(2050)$. Here, the theoretical results are obtained by taking $R = 4.0 - 7.0 \text{ GeV}^{-1}$.

Ratios	This work	Experiment
$\Gamma_{KK} / \Gamma_{\pi\pi}$	0.019 – 0.025	$0.04^{+0.02}_{-0.01}$ [19]
$\Gamma_{\pi\pi} / \Gamma_{Total}$	0.006 – 0.036	0.170 ± 0.015 [1]
$\Gamma_{\omega\omega} / \Gamma_{\pi\pi}$	3.9 – 21	1.5 ± 0.3 [19]
$\Gamma_{\eta\eta} / \Gamma_{Total}$	$(0.25 - 1.3) \times 10^{-3}$	$(2.1 \pm 0.8) \times 10^{-3}$ [18]

of $f_4(1^3F_4)$ and $f_4(2^3F_4)$, respectively.

As the isospin partners of $f_4(2050)$ and $f_4(2300)$, the decay features of $a_4(2040)$ and $a_4(2255)$ are similar to those of $f_4(2050)$ and $f_4(2300)$, respectively. There exists overlap between the experimental and calculated results of the total decay width for $a_4(2040)$ when $R = 4.0 - 5.8 \text{ GeV}^{-1}$. $\rho\omega$ and πb_1 as the dominant decay channels of $a_4(2040)$ is given in Fig. 10. The ratio $\Gamma_{\pi\rho} / \Gamma_{\pi f_2} = 1.1 \pm 0.2 \pm 0.2$ was obtained in Ref. [16], which can be reproduced well by our calculation with the value 1.2 – 2.1. In addition, we obtain the partial widths of $a_4(2040)$ decaying into $\pi\rho$ and KK , i.e., $\Gamma_{a_4(2040) \rightarrow \pi\rho} = 19 - 57 \text{ MeV}$ and $\Gamma_{a_4(2040) \rightarrow KK} = 0.035 - 0.43 \text{ MeV}$, which deviate from the experimental data $\Gamma_{a_4(2040) \rightarrow \pi\rho} = 10 \pm 3 \text{ MeV}$ and $\Gamma_{a_4(2040) \rightarrow KK} = 6 \pm 2 \text{ MeV}$, respectively in Ref. [85]. Thus, we also expect further experimental study of $a_4(2040)$.



There are two 6^{++} states, $f_6(2510)$ and its isospin partner $a_6(2450)$, which are treated as 1^3H_6 states. We calculate their partial and total decay widths which are presented in Fig. 11.

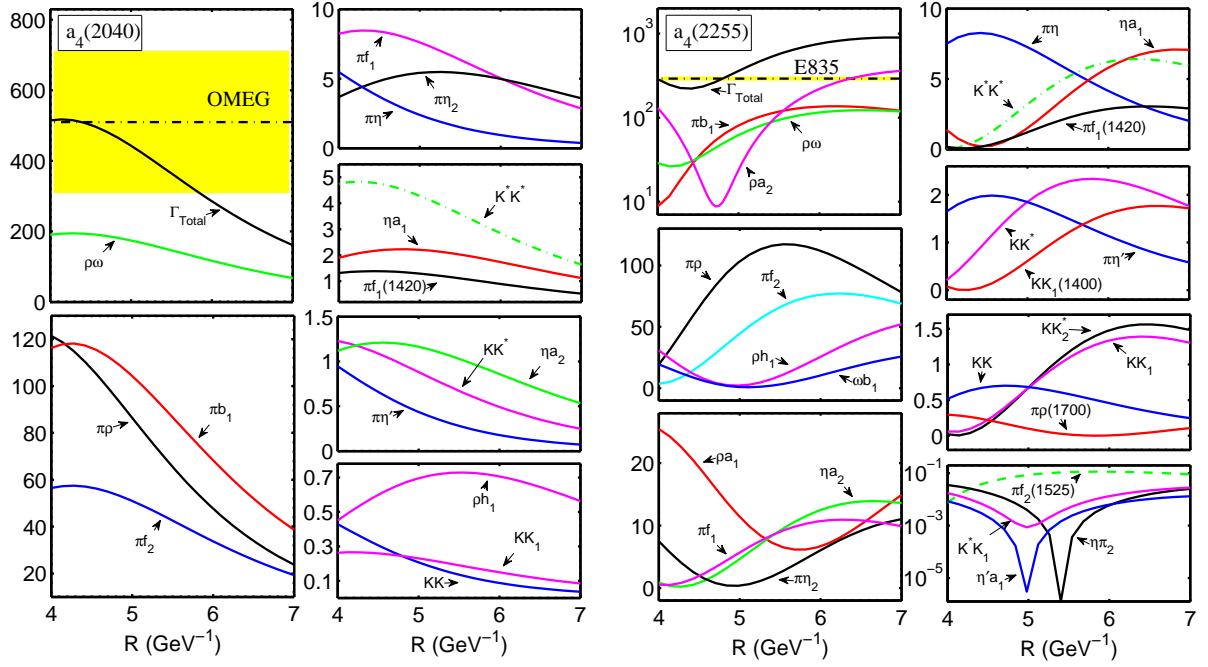


FIG. 10: (color online). The R dependence of the partial and total decay widths of $a_4(2040)$, and $a_4(2255)$. All results are in units of MeV. The dot-dashed lines with yellow bands are the corresponding experimental widths of $a_4(2040)$ [46], and $a_4(2255)$ [28].

D. Two 4^{-+} states

In this subsection, we discuss the last two observed high-spin states, $\eta_4(2330)$ and $\pi_4(2250)$, which have 4^{-+} quantum numbers (see Table I). The corresponding analysis of Regge trajectories with the $J-M^2$ plot is shown in Fig. 12 (b) which was used to study 2^{-+} states in our previous work [89]. π and π_2 [89] are the ground states of their own families. Thus, Fig. 12 (b) indicates that $\eta_4(2330)/\pi_4(2250)$ are the ground states of the η_4/π_4 meson families. In fact, Refs. [4, 34, 45, 84] gave the same suggestion. In the following, we calculate their two-body strong decays with the assignments $\eta_4(1^1G_4)$ and $\pi_4(1^1G_4)$ to $\eta_4(2330)$ and $\pi_4(2250)$, respectively.

Our calculated theoretical total width of $\eta_4(2330)$ is larger than the experimental data [2], where the main decay channels are ρb_1 , $\rho\rho$ and πa_2 , while πa_1 , ωh_1 , $\omega\omega$, and ηf_2 are its important decay channels. $\eta_4(2330)$ was first reported in the final states $(\pi a_2)_{L=4}$ and $(a_0\pi)_{L=4}$ and also observed in the ηf_2 channel [11]. The information of its partial decay width shows that $\eta_4(2330)$ as 1^1G_4 is reasonable. At present, a crucial task is to further check the resonance parameters of $\eta_4(2330)$.

Fig. 15 also present the decays of $\pi_4(2250)$. We find the theoretical total width is larger than the SPEC data [7] if taking the $R = 4 - 7 \text{ GeV}^{-1}$ range. $\pi_4(2250)$ mainly decays into $\rho\omega$, ρa_2 , ρh_1 and ρa_1 .

Before closing this section, we further list some important ratios in Table III, where the corresponding R values which can be adopted to reproduce the experimental data are collected.

IV. CONCLUSIONS AND DISCUSSION

In this work, we have mainly focused on the study of 26 high-spin states reported in experiments, where we have performed the mass spectrum analysis and have carried out the calculation of their two-body OZI-allowed strong decays, which is helpful to reveal their underlying features. The first task is to explore whether the observed high-spin states can be categorized into conventional meson families.

The analysis of Regge trajectories with the $n-M^2$ and $J-M^2$ plots has provided an effective approach to phenomenologically study the meson categorization. We have discussed the possible meson assignments to the observed high-spin states listed in PDG [1]. The main task of the present work has been the calculation of the two-body OZI-allowed strong decays of the high-spin states, which can be applied to test the possible meson assignments. In Sec. III, we have already given detailed discussion on this point. The predicted decay behaviors of the high-spin states under discussion can provide valuable information for their further experimental study in future.

At present, most of high-spin states reported in experiments are collected into the further state in PDG [1], since the experimental information of these high-spin unflavored states is not abundant. Thus, we suggest to have more experimental measurements of the resonance parameters and to search for the missing main decay channels. These efforts are helpful to establish these high-spin states in experiments.

With the experimental progress, exploring high-spin mesons is becoming an important issue of hadron physics. The BESIII, BelleII, and COMPASS experiments are good

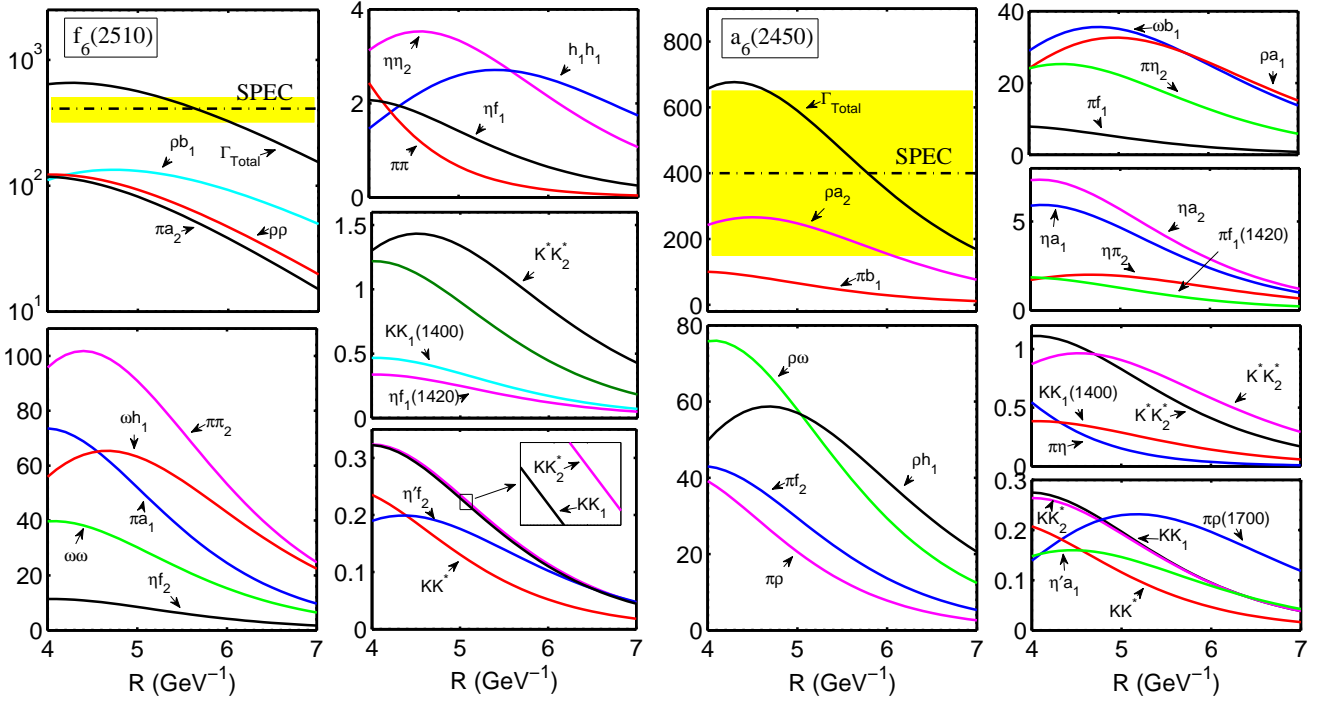


FIG. 11: (color online). The R dependence of the partial and total decay widths of $f_6(2510)$ and $a_6(2450)$ states. All results are in units of MeV. The dot-dashed lines with yellow bands are experimental widths of $f_6(2510)$ [2] and $a_6(2450)$ [25].

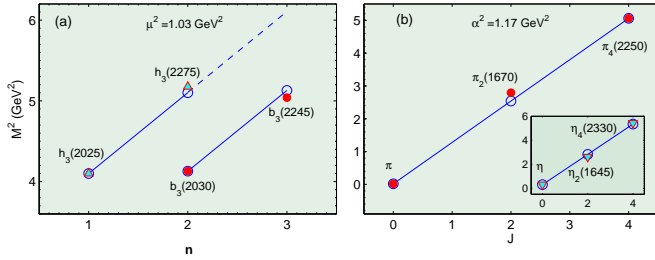


FIG. 12: (color online). The analysis of Regge trajectories for the observed states with the 3^{+-} and J^{++} quantum numbers. A diagram (a) is the n - M^2 plot for the 3^{+-} states, while a diagram (b) is the corresponding J - M^2 plot for the J^{++} states. For a diagram (a), a n - M^2 trajectory with $I = 1$ is displaced one unit to the right in n in order to resolve it from $I = 0$.

platforms. Inspired by this work, we hope to have more experimental and theoretical studies of high-spin states.

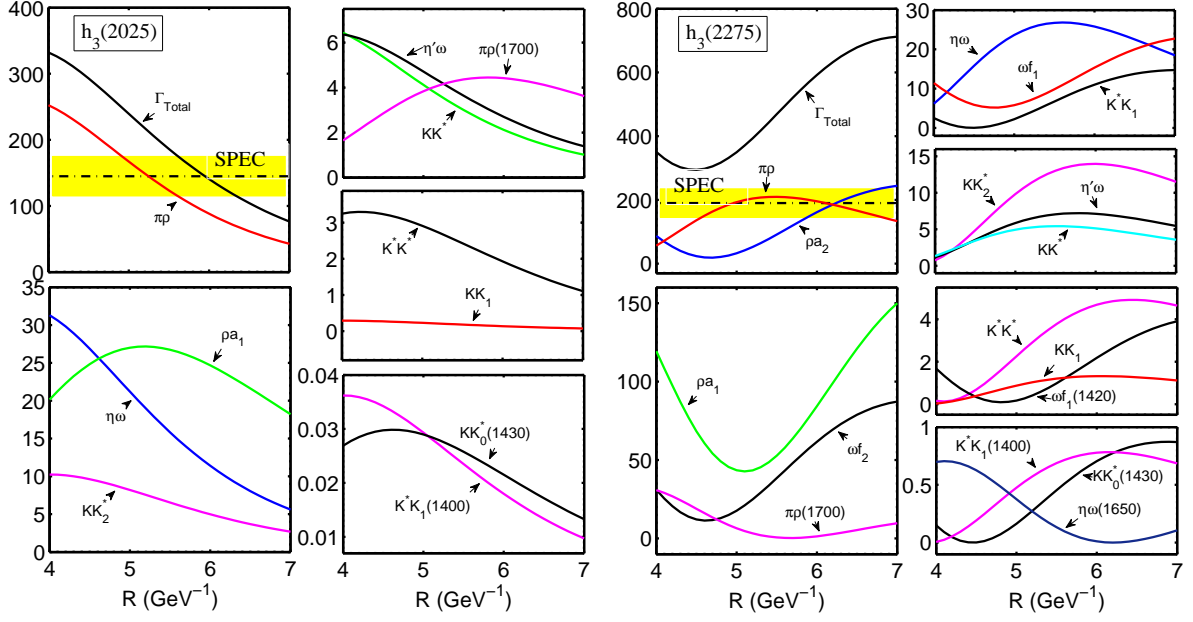


FIG. 13: (color online). The R dependence of the partial and total decay widths of $h_3(2025)$ and $h_3(2275)$ family. All results are in units of MeV. The dot-dashed lines with yellow bands are the corresponding experimental widths of $h_3(2025)$ and $h_3(2275)$ [9].

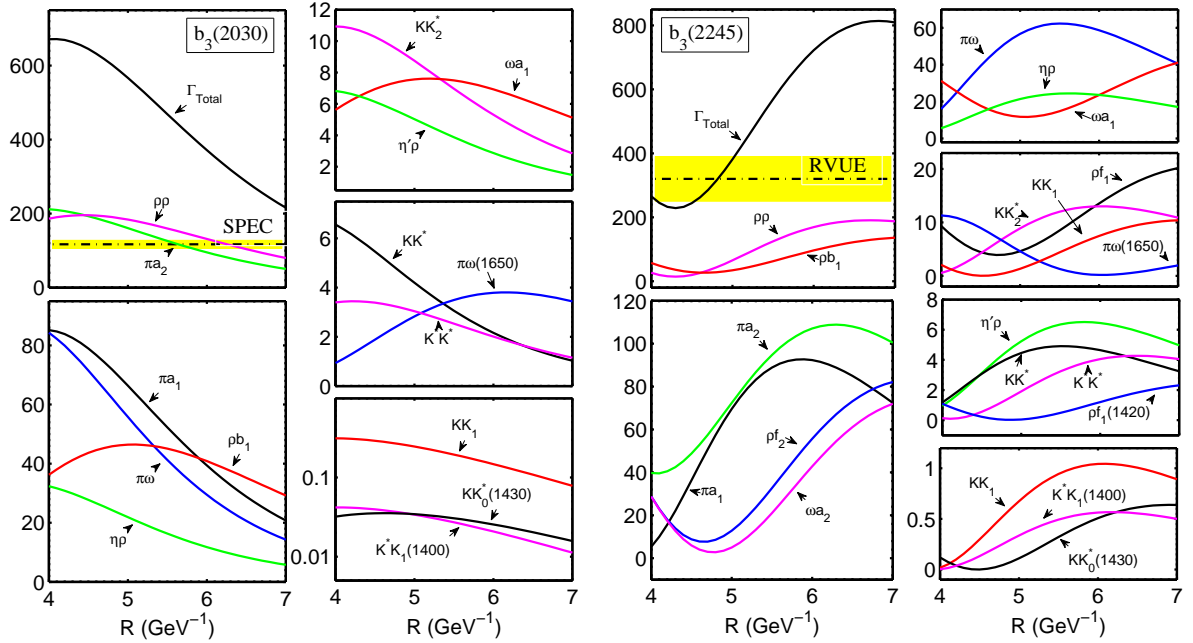


FIG. 14: (color online). The R dependence of the partial and total decay widths of $b_3(2030)$, and $h_3(2245)$ family. All results are in units of MeV. The dot-dashed lines with yellow bands are the corresponding experimental widths of $b_3(2030)$ [10], and $b_3(2245)$ [11].

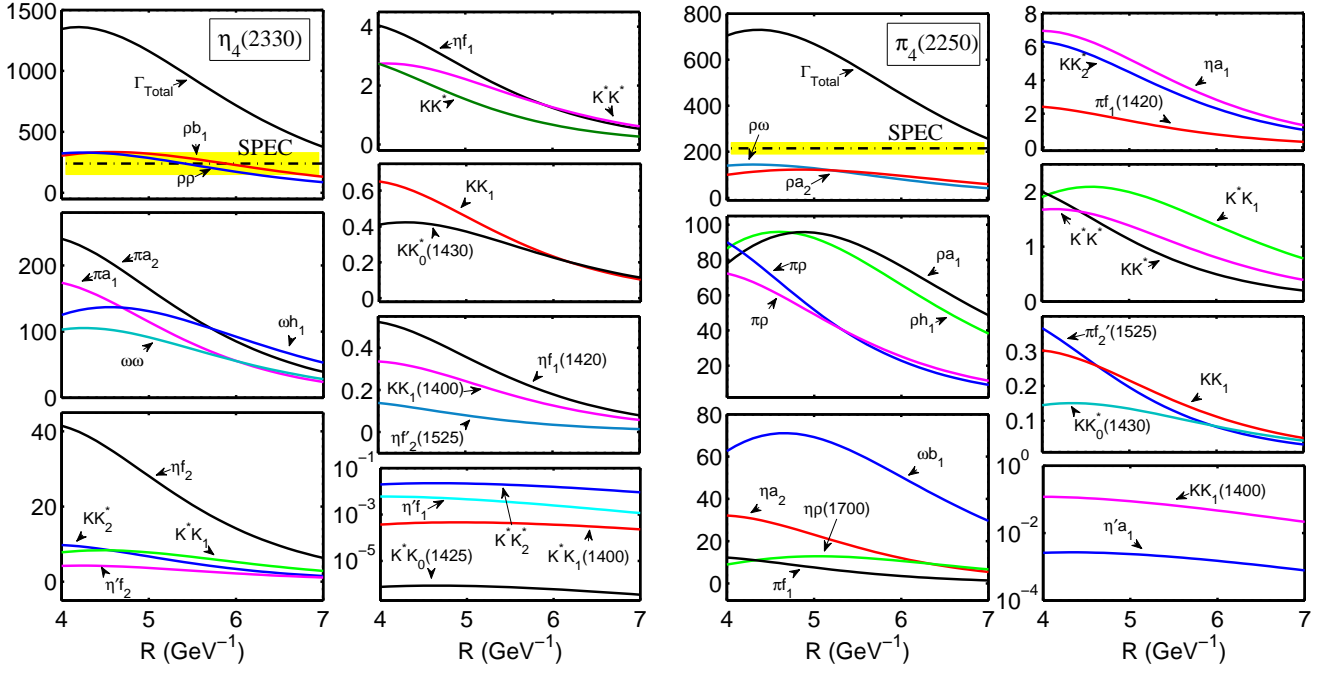


FIG. 15: (color online). The R dependence of the and total decay widths of $\pi_4(2250)$ and $\eta_4(2330)$ family. All results are in units of MeV. The dot-dashed lines with yellow bands are the corresponding experimental widths of $\pi_4(2250)$ [9] and $\eta_4(2330)$ [2].

TABLE III: The typical branching ratios of these discussed high-spin mesons corresponding to the successful R values.

States	R (GeV^{-1})	Ratios
$a_3(1875)$	4 – 4.6	$\Gamma_{\pi f_2}/\Gamma_{Total} = 0.33 - 0.34$, $\Gamma_{\pi\rho}/\Gamma_{Total} = 0.3 - 0.33$, $\Gamma_{\pi\rho}/\Gamma_{\pi f_2} = 0.91 - 0.98$, $\Gamma_{\rho\omega}/\Gamma_{Total} = 0.22 - 0.27$
$a_3(2030)$	4 – 7	$\Gamma_{\rho\omega}/\Gamma_{Total} = 0.26 - 0.32$, $\Gamma_{\rho h_1}/\Gamma_{\rho\omega} = 0.53 - 0.75$, $\Gamma_{\pi f_2}/\Gamma_{\pi\rho} = 0.41 - 0.51$, $\Gamma_{\eta a_2}/\Gamma_{Total} = 0.065 - 0.087$
$a_3(2275)$	4.6 – 5	$\Gamma_{\rho a_1}/\Gamma_{Total} = 0.066 - 0.077$, $\Gamma_{\pi\rho}/\Gamma_{Total} = 0.23 - 0.27$, $\Gamma_{\pi\rho}/\Gamma_{\rho a_1} = 3.3 - 3.8$, $\Gamma_{\rho h_1}/\Gamma_{Total} = 0.075 - 0.099$
$\omega_3(1670)$	4.0 – 5.4	$\Gamma_{\pi\rho}/\Gamma_{Total} = 0.69 - 0.75$, $\Gamma_{\pi b_1}/\Gamma_{Total} = 0.2 - 0.26$, $\Gamma_{\eta\omega}/\Gamma_{Total} = 0.035 - 0.036$, $\Gamma_{\eta\omega}/\Gamma_{\pi\rho} = 0.046 - 0.051$, $\Gamma_{\eta\omega}/\Gamma_{\pi b_1} = 0.13 - 0.17$, $\Gamma_{KK^*}/\Gamma_{Total} = 0.0028 - 0.0032$
$\omega_3(1945)$	5.3 – 7.0	$\Gamma_{\pi\rho}/\Gamma_{Total} = 0.81 - 0.84$, $\Gamma_{\pi b_1}/\Gamma_{Total} = 0.073 - 0.092$, $\Gamma_{\pi b_1}/\Gamma_{\pi\rho} = 0.087 - 0.11$, $\Gamma_{\eta\omega}/\Gamma_{Total} = 0.05 - 0.056$, $\Gamma_{\eta\omega}/\Gamma_{\pi\rho} = 0.059 - 0.068$, $\Gamma_{\eta\omega}/\Gamma_{\pi b_1} = 0.6 - 0.69$
$\phi_3(1850)$	5.3 – 7.0	$\Gamma_{K^*K^*}/\Gamma_{Total} = 0.59 - 0.65$, $\Gamma_{KK^*}/\Gamma_{Total} = 0.24 - 0.27$, $\Gamma_{KK^*}/\Gamma_{K^*K^*} = 0.36 - 0.46$
$\omega_3(2285)$	4.7 – 5.0	$\Gamma_{\pi\rho}/\Gamma_{Total} = 0.7 - 0.71$, $\Gamma_{\pi b_1}/\Gamma_{Total} = 0.13 - 0.13$, $\Gamma_{\pi b_1}/\Gamma_{\pi\rho} = 0.18 - 0.19$, $\Gamma_{\eta\omega}/\Gamma_{Total} = 0.059 - 0.065$, $\Gamma_{\eta\omega}/\Gamma_{\pi\rho} = 0.083 - 0.092$, $\Gamma_{\eta\omega}/\Gamma_{\pi b_1} = 0.47 - 0.49$, $\Gamma_{\rho a_1}/\Gamma_{Total} = 0.019 - 0.031$, $\Gamma_{\rho a_1}/\Gamma_{\pi\rho} = 0.027 - 0.044$
$\omega_3(2255)$	6.2 – 7.0	$\Gamma_{\rho a_1}/\Gamma_{Total} = 0.27 - 0.36$, $\Gamma_{\rho a_2}/\Gamma_{\rho a_1} = 0.68 - 0.84$, $\Gamma_{\omega f_2}/\Gamma_{Total} = 0.088 - 0.14$, $\Gamma_{\omega f_2}/\Gamma_{\rho a_1} = 0.32 - 0.38$, $\Gamma_{\omega f_2}/\Gamma_{\rho a_2} = 0.45 - 0.48$, $\Gamma_{\pi b_1}/\Gamma_{\pi\rho} = 0.33 - 0.47$, $\Gamma_{\pi\rho(1700)}/\Gamma_{Total} = 0.043 - 0.052$, $\Gamma_{\pi\rho(1700)}/\Gamma_{\rho a_1} = 0.14 - 0.16$
$f_4(2050)$	4 – 7	$\Gamma_{\rho\rho}/\Gamma_{Total} = 0.43 - 0.45$, $\Gamma_{\pi a_2}/\Gamma_{Total} = 0.22$, $\Gamma_{\pi a_2}/\Gamma_{\rho\rho} = 0.49 - 0.5$ $\Gamma_{\omega\omega}/\Gamma_{Total} = 0.14 - 0.15$, $\Gamma_{\omega\omega}/\Gamma_{\rho\rho} = 0.33$, $\Gamma_{\omega\omega}/\Gamma_{\pi a_2} = 0.66$
$f_4(2300)$	4.0 – 7.0	$\Gamma_{\pi a_2}/\Gamma_{Total} = 0.020 - 0.25$, $\Gamma_{\rho\rho}/\Gamma_{Total} = 0.092 - 0.21$, $\Gamma_{\rho\rho}/\Gamma_{\pi a_2} = 0.77 - 4.3$, $\Gamma_{\pi a_1}/\Gamma_{Total} = 0.020 - 0.075$
$a_4(2040)$	4.0 – 5.8	$\Gamma_{\rho\omega}/\Gamma_{Total} = 0.36 - 0.38$, $\Gamma_{\pi\rho}/\Gamma_{Total} = 0.16 - 0.23$, $\Gamma_{\pi\rho}/\Gamma_{\rho\omega} = 0.42 - 0.64$, $\Gamma_{\pi b_1}/\Gamma_{Total} = 0.22$, $\Gamma_{\pi b_1}/\Gamma_{\rho\omega} = 0.59 - 0.61$, $\Gamma_{\pi b_1}/\Gamma_{\pi\rho} = 0.96 - 1.4$, $\Gamma_{\pi f_2}/\Gamma_{Total} = 0.11$, $\Gamma_{\pi f_2}/\Gamma_{\rho\omega} = 0.29 - 0.3$
$a_4(2255)$	4.7 – 4.8	$\Gamma_{\pi f_2}/\Gamma_{\pi b_1} = 0.41 - 0.57$, $\Gamma_{\pi f_1}/\Gamma_{\pi f_2} = 0.092 - 0.14$, $\Gamma_{\pi\eta'}/\Gamma_{\pi\eta} = 0.22 - 0.29$
$\pi_4(2250)$	4.0 – 7.0	$\Gamma_{\rho\omega}/\Gamma_{Total} = 0.15 - 0.19$, $\Gamma_{\rho a_2}/\Gamma_{Total} = 0.14 - 0.23$, $\Gamma_{\rho h_1}/\Gamma_{Total} = 0.12 - 0.15$, $\Gamma_{\rho h_1}/\Gamma_{\rho\omega} = 0.62 - 0.92$, $\Gamma_{\rho h_1}/\Gamma_{\rho a_2} = 0.64 - 0.87$, $\Gamma_{\rho a_1}/\Gamma_{\rho a_2} = 0.78 - 0.82$, $\Gamma_{\rho a_1}/\Gamma_{\rho h_1} = 0.9 - 1.3$, $\Gamma_{\pi f_2}/\Gamma_{\pi\rho} = 0.8 - 1.3$
$\eta_4(2330)$	4.0 – 7.0	$\Gamma_{\rho b_1}/\Gamma_{Total} = 0.23 - 0.35$, $\Gamma_{\rho\rho}/\Gamma_{Total} = 0.23 - 0.25$, $\Gamma_{\pi a_2}/\Gamma_{\rho\rho} = 0.45 - 0.74$, $\Gamma_{\pi a_1}/\Gamma_{\pi a_2} = 0.61 - 0.72$, $\Gamma_{\omega h_1}/\Gamma_{Total} = 0.093 - 0.14$, $\Gamma_{\omega h_1}/\Gamma_{\rho b_1} = 0.4 - 0.41$, $\Gamma_{\omega h_1}/\Gamma_{\rho\rho} = 0.39 - 0.61$, $\Gamma_{\omega\omega}/\Gamma_{Total} = 0.075 - 0.079$
$\rho_4(2230)$	6.8 – 7	$\Gamma_{\rho\rho}/\Gamma_{Total} = 0.2 - 0.21$, $\Gamma_{\rho b_1}/\Gamma_{Total} = 0.19 - 0.27$, $\Gamma_{\rho b_1}/\Gamma_{\rho\rho} = 0.92 - 1.3$, $\Gamma_{\pi a_1}/\Gamma_{Total} = 0.094 - 0.12$, $\Gamma_{\pi a_1}/\Gamma_{\rho\rho} = 0.46 - 0.60$, $\Gamma_{\rho f_2}/\Gamma_{\rho b_1} = 0.3 - 0.39$, $\Gamma_{\omega a_1}/\Gamma_{\rho b_1} = 0.29 - 0.33$
$\omega_4(2250)$	4 – 7	$\Gamma_{\rho a_1}/\Gamma_{Total} = 0.27 - 0.36$, $\Gamma_{\rho a_2}/\Gamma_{\rho a_1} = 0.68 - 0.84$, $\Gamma_{\omega f_2}/\Gamma_{Total} = 0.088 - 0.14$, $\Gamma_{\omega f_2}/\Gamma_{\rho a_1} = 0.32 - 0.38$, $\Gamma_{\omega f_2}/\Gamma_{\rho a_2} = 0.45 - 0.48$, $\Gamma_{\pi b_1}/\Gamma_{\pi\rho} = 0.33 - 0.47$, $\Gamma_{\pi\rho(1700)}/\Gamma_{Total} = 0.043 - 0.052$, $\Gamma_{\pi\rho(1700)}/\Gamma_{\rho a_1} = 0.14 - 0.16$
$\omega_5(22250)$	4 – 7	$\Gamma_{\rho a_2}/\Gamma_{Total} = 0.42 - 0.58$, $\Gamma_{\omega f_2}/\Gamma_{Total} = 0.19 - 0.23$, $\Gamma_{\omega f_2}/\Gamma_{\rho a_2} = 0.4 - 0.45$, $\Gamma_{\pi\rho}/\Gamma_{\pi b_1} = 0.35 - 0.57$, $\Gamma_{\eta h_1}/\Gamma_{\pi b_1} = 0.1 - 0.12$, $\Gamma_{\eta\omega}/\Gamma_{\pi b_1} = 0.042 - 0.058$, $\Gamma_{\eta\omega}/\Gamma_{\pi\rho} = 0.1 - 0.12$, $\Gamma_{\eta\omega}/\Gamma_{\eta h_1} = 0.35 - 0.58$
$\rho_5(2350)$	4.0 – 7.0	$\Gamma_{\rho f_2}/\Gamma_{Total} = 0.20 - 0.21$, $\Gamma_{\omega a_2}/\Gamma_{Total} = 0.17 - 0.24$, $\Gamma_{\omega a_2}/\Gamma_{\rho f_2} = 0.86 - 1$, $\Gamma_{\rho\rho}/\Gamma_{Total} = 0.087 - 0.12$, $\Gamma_{\pi a_2}/\Gamma_{\rho\rho} = 0.82 - 0.99$, $\Gamma_{\pi h_1}/\Gamma_{\rho\rho} = 0.53 - 0.78$, $\Gamma_{\pi h_1}/\Gamma_{\pi a_2} = 0.64 - 0.78$, $\Gamma_{\rho b_1}/\Gamma_{\rho f_2} = 0.33 - 0.54$
$f_6(2510)$	6 – 6.4	$\Gamma_{\rho b_1}/\Gamma_{Total} = 0.28 - 0.3$, $\Gamma_{\rho\rho}/\Gamma_{Total} = 0.14 - 0.14$, $\Gamma_{\rho\rho}/\Gamma_{\rho b_1} = 0.46 - 0.51$, $\Gamma_{\pi a_2}/\Gamma_{Total} = 0.11 - 0.12$, $\Gamma_{\pi a_2}/\Gamma_{\rho b_1} = 0.36 - 0.41$, $\Gamma_{\pi a_2}/\Gamma_{\rho\rho} = 0.79 - 0.81$, $\Gamma_{\pi\pi_2}/\Gamma_{Total} = 0.16$, $\Gamma_{\pi\pi_2}/\Gamma_{\rho b_1} = 0.54 - 0.58$
$a_6(2450)$	4 – 7	$\Gamma_{\rho a_2}/\Gamma_{Total} = 0.37 - 0.46$, $\Gamma_{\rho\omega}/\Gamma_{Total} = 0.074 - 0.12$, $\Gamma_{\rho\omega}/\Gamma_{\pi b_1} = 0.75 - 1.1$, $\Gamma_{\rho h_1}/\Gamma_{Total} = 0.076 - 0.12$, $\Gamma_{\rho h_1}/\Gamma_{\rho a_2} = 0.21 - 0.27$, $\Gamma_{\pi f_2}/\Gamma_{\pi b_1} = 0.43 - 0.48$, $\Gamma_{\pi f_2}/\Gamma_{\rho\omega} = 0.43 - 0.57$, $\Gamma_{\pi\rho}/\Gamma_{\pi b_1} = 0.24 - 0.39$

Acknowledgments

This project is supported by the National Science Foundation for Fostering Talents in Basic Research of the National Natural Science Foundation of China and the National Natural

Science Foundation of China under Grants No. 11222547 and No. 11175073, the Ministry of Education of China (SRFDP under Grant No. 2012021111000), and the Fok Ying Tung Education Foundation (Grant No. 131006).

-
- [1] K. A. Olive *et al.* [Particle Data Group Collaboration], *Chin. Revs. C* **38**, 090001 (2014).
 - [2] A. V. Anisovich, C. A. Baker, C. J. Batty, D. V. Bugg, C. Hodde, H. C. Lu, V. A. Nikonov and A. V. Sarantsev *et al.*, *Phys. Lett. B* **491**, 47 (2000) [arXiv:1109.0883 [hep-ex]].
 - [3] D. V. Bugg, *Eur. Phys. J. C* **36**, 161 (2004) [hep-ph/0406292].
 - [4] S. S. Afonin, *Phys. Rev. C* **76**, 015202 (2007) [arXiv:0707.0824 [hep-ph]].
 - [5] P. Masjuan, E. R. Arriola and W. Broniowski, *Phys. Rev. D* **85**, 094006 (2012) [arXiv:1203.4782 [hep-ph]].
 - [6] D. Ebert, R. N. Faustov and V. O. Galkin, *Phys. Rev. D* **79**, 114029 (2009) [arXiv:0903.5183 [hep-ph]].
 - [7] A. V. Anisovich, C. A. Baker, C. J. Batty, D. V. Bugg, V. A. Nikonov, A. V. Sarantsev, V. V. Sarantsev and B. S. Zou, *Phys. Lett. B* **517**, 261 (2001) [arXiv:1110.0278 [hep-ex]].
 - [8] A. V. Anisovich, C. A. Baker, C. J. Batty, D. V. Bugg, V. A. Nikonov, A. V. Sarantsev, V. V. Sarantsev and B. S. Zou, *Phys. Lett. B* **517**, 273 (2001) [arXiv:1109.6817 [hep-ex]].
 - [9] A. V. Anisovich, C. A. Baker, C. J. Batty, D. V. Bugg, L. Montanet, V. A. Nikonov, A. V. Sarantsev and V. V. Sarantsev *et al.*, *Phys. Lett. B* **542**, 19 (2002) [arXiv:1109.5817 [hep-ex]].
 - [10] A. V. Anisovich, C. A. Baker, C. J. Batty, D. V. Bugg, L. Montanet, V. A. Nikonov, A. V. Sarantsev and V. V. Sarantsev *et al.*, *Phys. Lett. B* **542**, 8 (2002) [arXiv:1109.5247 [hep-ex]].
 - [11] D. V. Bugg, *Phys. Rept.* **397**, 257 (2004) [hep-ex/0412045].
 - [12] L. -P. He, X. Wang and X. Liu, *Phys. Rev. D* **88**, no. 3, 034008 (2013) [arXiv:1306.5562 [hep-ph]].
 - [13] J. Diaz, F. A. Dibiaccia, W. J. Fickinger, J. A. Malko, D. K. Robinson, C. R. Sullivan, J. C. Anderson and A. Engler *et al.*, *Phys. Rev. Lett.* **32**, 260 (1974).
 - [14] M. Baubillier *et al.* [Birmingham-CERN-Glasgow-Michigan State-Paris Collaboration], *Phys. Lett. B* **89**, 131 (1979).
 - [15] D. Aston, N. Awaji, T. Bienz, F. Bird, J. D'Amore, W. M. Dunwoodie, R. Endorf and K. Fujii *et al.*, *Phys. Lett. B* **208**, 324 (1988).
 - [16] S. U. Chung, K. Danyo, R. W. Hackenburg, C. Olchanski, J. S. Suh, H. J. Willutzki, S. P. Denisov and V. Dorofeev *et al.*, *Phys. Rev. D* **65**, 072001 (2002).
 - [17] D. Alde *et al.* [IHEP-IISN-LANL-LAPP-TSUIHEP Collaboration], *Phys. Lett. B* **241**, 600 (1990).
 - [18] D. Alde *et al.* [Serpukhov-Brussels-Los Alamos-Anneecy(LAPP) Collaboration], *Nucl. Phys. B* **269**, 485 (1986).
 - [19] A. Etkin, K. J. Foley, R. S. Longacre, W. A. Love, T. W. Morris, S. Ozaki, E. D. Platner and V. A. Polychronakos *et al.*, *Phys. Rev. D* **25**, 1786 (1982).
 - [20] D. Barberis *et al.* [WA102 Collaboration], *Phys. Lett. B* **484**, 198 (2000) [hep-ex/0005027].
 - [21] D. Cutts, M. L. Good, P. D. Grannis, D. Green, Y. Y. Lee, R. Pittman, J. Storer and A. C. Benvenuti *et al.*, *Phys. Rev. D* **17**, 16 (1978).
 - [22] A. A. Carter, M. Coupland, E. Eisenhandler, W. R. Gibson, P. I. P. Kalmus, D. P. Kimber, A. Astbury and D. P. Jones, *Phys. Lett. B* **67**, 117 (1977).
 - [23] A. Hasan and D. V. Bugg, *Phys. Lett. B* **334**, 215 (1994).
 - [24] D. V. Amelin *et al.* [VES Collaboration], *Nucl. Phys. A* **668**, 83 (2000).
 - [25] W. E. Cleland, A. Delfosse, P. a. Dorsaz, J. I. Gloor, M. n. Kienzle-Focacci, G. Mancarella, A. D. Martin and M. Martin *et al.*, *Nucl. Phys. B* **208**, 228 (1982).
 - [26] R. Baldi, T. Bohringer, P. A. Dorsaz, V. Hungerbuhler, M. N. Kienzle-Focacci, M. Martin, A. Mermoud and C. Nef *et al.*, *Phys. Lett. B* **74**, 413 (1978).
 - [27] M. Lu *et al.* [E852 Collaboration], *Phys. Rev. Lett.* **94**, 032002 (2005) [hep-ex/0405044].
 - [28] I. Uman, D. Joffe, Z. Metreveli, K. K. Seth, A. Tomaradze and P. K. Zweber, *Phys. Rev. D* **73**, 052009 (2006) [hep-ex/0607034].
 - [29] D. Alde *et al.* [GAMS Collaboration], *Phys. Atom. Nucl.* **59**, 982 (1996) [*Yad. Fiz.* **59N6**, 1027 (1996)].
 - [30] E. I. Ivanov *et al.* [E852 Collaboration], *Phys. Rev. Lett.* **86**, 3977 (2001) [hep-ex/0101058].
 - [31] R. J. Abrams, R. L. Cool, G. Giacomelli, T. F. Kycia, B. A. Leontic, K. K. Li and D. N. Michael, *Phys. Rev. Lett.* **18**, 1209 (1967).
 - [32] B. Alper *et al.* [Amsterdam-CERN-Cracow-Munich-Oxford-Rutherford Collaboration], *Phys. Lett. B* **94**, 422 (1980).
 - [33] F. G. Binon *et al.* [Serpukhov-Brussels-Anneecy(LAPP) Collaboration], *Lett. Nuovo Cim.* **39**, 41 (1984) [*Yad. Fiz.* **38**, 1199 (1983)] [*Sov. J. Nucl. Phys.* **38**, 723 (1983)].
 - [34] V. V. Anisovich, *Phys. Usp.* **47**, 45 (2004) [*Usp. Fiz. Nauk* **47**, 49 (2004)] [hep-ph/0208123].
 - [35] V. V. Anisovich, *AIP Conf. Proc.* **717**, 441 (2004) [hep-ph/0310165].
 - [36] N. Armenise, A. Forino and A. M. Cartacci, *Phys. Lett. B* **26**, 336 (1968).
 - [37] S. Al-Harran *et al.* [BIRMINGHAM-CERN-GLASGOW-MICHIGAN STATE-PARIS Collaboration], *Phys. Lett. B* **101**, 357 (1981).
 - [38] T. Armstrong *et al.* [BARI-BIRMINGHAM-CERN-MILAN-PARIS-PAVIA Collaboration], *Phys. Lett. B* **110**, 77 (1982).
 - [39] W. D. Apel *et al.* [Serpukhov-CERN Collaboration], *Phys. Lett. B* **57**, 398 (1975).
 - [40] W. Blum *et al.* [CERN-MUNICH Collaboration], *Phys. Lett. B* **57**, 403 (1975).
 - [41] R. J. Abrams, R. L. Cool, G. Giacomelli, T. F. Kycia, B. A. Leontic, K. K. Li and D. N. Michael, *Phys. Rev. D* **1**, 1917 (1970).
 - [42] A. A. Carter, *Nucl. Phys. B* **141**, 467 (1978).
 - [43] R. S. Dulude, R. E. Lanou, J. T. Massimo, D. C. Peaslee, R. K. Thornton, D. S. Barton, M. Marx and B. A. Nelson *et al.*, *Phys. Lett. B* **79**, 335 (1978).
 - [44] L. Roca and E. Oset, *Phys. Rev. D* **82**, 054013 (2010) [arXiv:1005.0283 [hep-ph]].
 - [45] A. V. Anisovich, V. V. Anisovich and A. V. Sarantsev, *Phys. Rev. D* **62**, 051502 (2000) [hep-ph/0003113].
 - [46] M. J. Corden, J. D. Dowell, J. Garvey, M. Jobs, I. R. Kenyon, J. Mawson, T. McMahon and I. F. Corbett *et al.*, *Nucl. Phys. B*

- 136**, 77 (1978).
- [47] D. V. Amelin *et al.* [VES Collaboration], Phys. Atom. Nucl. **62**, 445 (1999) [Yad. Fiz. **62**, 487 (1999)].
 - [48] B. R. Martin and D. Morgan, Nucl. Phys. B **176**, 355 (1980).
 - [49] D. Alde *et al.* [GAMS Collaboration], Nuovo Cim. A **107**, 1867 (1994) [Z. Phys. C **66**, 379 (1995)].
 - [50] V. N. Bolotov, V. V. Isakov, D. B. Kakauridze, G. V. Khaustov, Y. D. Prokoshkin and S. A. Sadovsky, Phys. Lett. B **52**, 489 (1974) [Sov. J. Nucl. Phys. **20**, 635 (1975)] [Yad. Fiz. **20**, 1214 (1974)].
 - [51] D. Alde *et al.* [GAMS Collaboration], Eur. Phys. J. A **3**, 361 (1998).
 - [52] A. A. Tseytlin, Phys. Lett. B **208**, 228 (1988).
 - [53] L. Y. Glozman and A. V. Nefediev, Phys. Rev. D **76**, 096004 (2007) [arXiv:0704.2673 [hep-ph]].
 - [54] L. Y. Glozman, Phys. Rept. **444**, 1 (2007) [hep-ph/0701081].
 - [55] L. Y. Glozman, Eur. Phys. J. A **51**, no. 3, 27 (2015) [arXiv:1407.2798 [hep-ph]].
 - [56] S. S. Afonin, Eur. Phys. J. A **29**, 327 (2006) [hep-ph/0606310].
 - [57] L. Micu, Nucl. Phys. B **10**, 521 (1969).
 - [58] A. Le Yaouanc, L. Oliver, O. Pene and J. C. Raynal, Phys. Rev. D **8**, 2223 (1973).
 - [59] A. Le Yaouanc, L. Oliver, O. Pene and J. -C. Raynal, Phys. Rev. D **9**, 1415 (1974).
 - [60] A. Le Yaouanc, L. Oliver, O. Pene and J. C. Raynal, Phys. Rev. D **11**, 1272 (1975).
 - [61] A. Le Yaouanc, L. Oliver, O. Pene and J. -C. Raynal, Phys. Lett. B **71**, 397 (1977).
 - [62] A. Le Yaouanc, L. Oliver, O. Pene and J. C. Raynal, Phys. Lett. B **72**, 57 (1977).
 - [63] E. van Beveren, G. Rupp, T. A. Rijken and C. Dullemond, Phys. Rev. D **27**, 1527 (1983).
 - [64] S. Capstick and W. Roberts, Phys. Rev. D **49**, 4570 (1994) [nucl-th/9310030].
 - [65] H. G. Blundell and S. Godfrey, Phys. Rev. D **53**, 3700 (1996) [hep-ph/9508264].
 - [66] E. S. Ackleh, T. Barnes and E. S. Swanson, Phys. Rev. D **54**, 6811 (1996) [hep-ph/9604355].
 - [67] S. Capstick and B. D. Keister, [nucl-th/9611055].
 - [68] F. E. Close and E. S. Swanson, Phys. Rev. D **72**, 094004 (2005) [hep-ph/0505206].
 - [69] B. Zhang, X. Liu, W. -Z. Deng and S. -L. Zhu, Eur. Phys. J. C **50**, 617 (2007) [hep-ph/0609013].
 - [70] J. Lu, W. -Z. Deng, X. -L. Chen and S. -L. Zhu, Phys. Rev. D **73**, 054012 (2006) [hep-ph/0602167].
 - [71] Z. -F. Sun and X. Liu, Phys. Rev. D **80**, 074037 (2009) [arXiv:0909.1658 [hep-ph]].
 - [72] X. Liu, Z. -G. Luo and Z. -F. Sun, Phys. Rev. Lett. **104**, 122001 (2010) [arXiv:0911.3694 [hep-ph]].
 - [73] Z. -F. Sun, J. -S. Yu, X. Liu and T. Matsuki, Phys. Rev. D **82**, 111501 (2010) [arXiv:1008.3120 [hep-ph]].
 - [74] T. A. Rijken, M. M. Nagels and Y. Yamamoto, Nucl. Phys. A **835**, 160 (2010).
 - [75] J. -S. Yu, Z. -F. Sun, X. Liu and Q. Zhao, Phys. Rev. D **83**, 114007 (2011) [arXiv:1104.3064 [hep-ph]].
 - [76] Z. -Y. Zhou and Z. Xiao, Phys. Rev. D **84**, 034023 (2011) [arXiv:1105.6025 [hep-ph]].
 - [77] Z. -C. Ye, X. Wang, X. Liu and Q. Zhao, Phys. Rev. D **86**, 054025 (2012) [arXiv:1206.0097 [hep-ph]].
 - [78] Y. Sun, X. Liu and T. Matsuki, Phys. Rev. D **88**, 094020 (2013) [arXiv:1309.2203 [hep-ph]].
 - [79] Y. Sun, Q. -T. Song, D. -Y. Chen, X. Liu and S. -L. Zhu, Phys. Rev. D **89**, 054026 (2014) [arXiv:1401.1595 [hep-ph]].
 - [80] W. Roberts and B. Silvestre-Brac, Acta Phys. Austriaca **11**, 171 (1992).
 - [81] H. G. Blundell, hep-ph/9608473.
 - [82] M. Jacob and G. C. Wick, Annals Phys. **7**, 404 (1959) [Annals Phys. **281**, 774 (2000)].
 - [83] M. J. Corden, J. D. Dowell, J. Garvey, M. Jobes, I. R. Kenyon, J. Mawson, T. McMahon and I. F. Corbett *et al.*, Nucl. Phys. B **138**, 235 (1978).
 - [84] E. Klempt and A. Zaitsev, Phys. Rept. **454**, 1 (2007) [arXiv:0708.4016 [hep-ph]].
 - [85] A. Bramon and E. Masso, Z. Phys. C **8**, 135 (1981).
 - [86] D. V. Bugg, Phys. Lett. B **572**, 1 (2003) [Erratum-ibid. B **595**, 556 (2004)].
 - [87] X. Wang, Z. F. Sun, D. Y. Chen, X. Liu and T. Matsuki, Phys. Rev. D **85**, 074024 (2012) [arXiv:1202.4139 [hep-ph]].
 - [88] K. Chen, C. Q. Pang, X. Liu and T. Matsuki, arXiv:1501.07766 [hep-ph].
 - [89] B. Wang, C. Q. Pang, X. Liu and T. Matsuki, Phys. Rev. D **91**, 014025 (2015) [arXiv:1410.3930 [hep-ph]].
 - [90] C. Q. Pang, L. P. He, X. Liu and T. Matsuki, Phys. Rev. D **90**, 014001 (2014) [arXiv:1405.3189 [hep-ph]].